A METHOD FOR PROPULSION NOZZLE DESIGN

by

Azim Eskandarian

Thesis submitted to the Graduate Faculty of the Virginia Polytechnic Institute and State University in partial fulfillment of requirements for the degree of

MASTER OF SCIENCE

in

Mechanical Engineering

APPROVED

E. F. Brown

F. J. Pierce

John Moore

October, 1983
Blacksburg, Virginia

A METHOD FOR PROPULSION NOZZLE DESIGN

by

Azim Eskandarian

(ABSTRACT)

An inverse method for the design of exhaust nozzles with a specified transonic pressure distribution is presented. A problem of mixed Neumann and Dirichlet boundary condition is solved. A successive line relaxation process is used to solve the array of velocity potentials in the entire flow field. The streamlines are then displaced to produce boundaries which match a desired pressure distribution. Various cases are tested to verify the reliability of the method. The design calculation proves to be efficient and accurate.

ACKNOWLEDGEMENTS

This work was conducted under a research contract with the Douglas Aircraft Company. I would like to thank Mrs. Eloise Lafon for typing the thesis.

I am also thankful to T. Brecht who developed the analysis portion of the program which is used in this thesis. Thanks are also due Professors F. J. Pierce and John Moore for their help. I am especially grateful to my adviser, Dr. Eugene F. Brown, for his advice and encouragement over the past year which resulted in the successful completion of this work.

TABLE OF CONTENTS

LIST OF FIGURES

LIST OF TABLES

NOMENCLATURE

A,B,C	Coefficients of the second derivatives in the governing equation
c	Speed of sound
D	Non-homogeneous term in transformed form of governing equation
F	Rotation function
F_r	Radial derivative of the rotation function
M	Mach number
n	Coordinate normal to streamline
P	Pressure
r	Radial coordinate in the physical plane
R_i	Inner wall radius (nondimensionalized with respect to the radius of the outer wall at the throat)
R_o	Outer wall radius (nondimensionalized with respect to the radius of the outer wall at the throat)
s	Coordinate along streamline
u	Axial velocity component (nondimensionalized with respect to the local stagnation speed of sound)
v	Radial velocity component (nondimensionalized with respect to the local stagnation speed of sound)
V	Velocity
V_s	Tangential velocity component on boundary (nondimensionalized with respect to the local stagnation speed of sound)
V_n	Normal velocity component on boundary (nondimensionalized with respect to the local stagnation speed of sound)
x	Axial coordinate in the physical plane (nondimensionalized with respect to the radius of the outer wall at the throat)
y	Lateral coordinate in the physical plane (for planar flow)
γ	Ratio of specific heats

Δs Spacing between two computational points along the boundary (physical plane)

$\Delta \xi$ Mesh spacing in axial direction (computational plane)

$\Delta \psi$ Mesh spacing in radial direction (computational plane)

θ Wall angle

$\Omega 1$ Displacement under-relaxation factor

$\Omega 2$ Displacement over-relaxation factor

ξ Axial coordinate in the computational plane

ρ Density

ϕ Velocity function

ψ Radial coordinate in the computational plane

ω Rotation

δ Displacement of the wall (or centerbody)

δ' Under/over-relaxed displacement of the wall (or centerbody)

Subscripts

$\mathcal{L}$ Centerline or inner wall

i Mesh point index in the axial direction (except when used with R)

imax Largest axial index

j Mesh point index in the radial direction

jmax Radial index at outer wall

r Radial derivative in the physical plane

x Axial derivative in the physical plane

ξ Axial derivative in the computational plane

ψ Radial derivative in the computatinal plane

o Stagnation conditions

Superscripts

New values after relaxation

1. INTRODUCTION

1.1 Problem Description

Accurate calculation of transonic flows is of special interest because many aerodynamic components operate in the transonic range. Among these components are jet propulsion exhaust nozzles which create thrust by accelerating exhaust gases to a high speed.

Alternative means for obtaining an optimum exhaust nozzle configuration can be categorized as 1) experimental and 2) computational methods. Experimental methods can be very costly and time consuming. Therefore, efficient design and development of exhaust nozzles requires capable computational methods.

Often it is desired to have a specified velocity or pressure distribution on the nozzle wall in order to control the forces and the boundary layer growth. Calculating the proper geometry of a nozzle which generates a prescribed pressure distribution is called a design (or inverse) method. This contrasts with calculating the characteristics of the flow field associated with a specified nozzle shape which is called an analysis method (1).

Brown, Brecht, and Walsh (2) obtained a successful analysis procedure to predict the flow field in propulsion-type nozzles including rotational flow effects. Without a design method, such analysis methods have to be repeatedly applied for a wide range of nozzle contour configurations until a suitable configuration is found. This repeated application is without good guidance, relying as it does completely upon

human judgement. Since this is not a systemetized procedure, it is wasteful in computer time. A well posed design method can overcome this problem and efficiently provide an optimum geometry.

A typical design method can be described as follows. The design calculation begins with a prescribed pressure distribution and a guess for the initial profile of the nozzle (It should be remembered at this point that the design calculations allow either the outer wall of the nozzle or the nozzle centerbody (inner wall) to be modified). The associated flow field is calculated by an analysis method to give a pressure distribution which is then compared with the desired pressure distribution. A design calculation is then initiated to modify the initial geometry. The modified geometry is again analyzed to find the corresponding pressure distribution. This iterative process between the design and analysis schemes continues until the shape of a nozzle is found which satisfies the design requirements.

This type of design calculation (in which the design and analysis methods are combined) has been developed for design of airfoils. Figures 1A and 1B show the application of such a method to a nozzle design problem. Figure 1A shows the initial (input) geometry, by the dashed lines, and Fig 1B shows the desired pressure variation along the wall of the nozzle by the solid line. The diamonds in Fig. 1B show the pressure distribution which corresponds to the input (initial) geometry. The design procedure results in the modification of the wall geometry to the configuration shown by the solid line in Fig. 1A, and the circles in Fig 1B show that the desired pressure ratio has been reached.

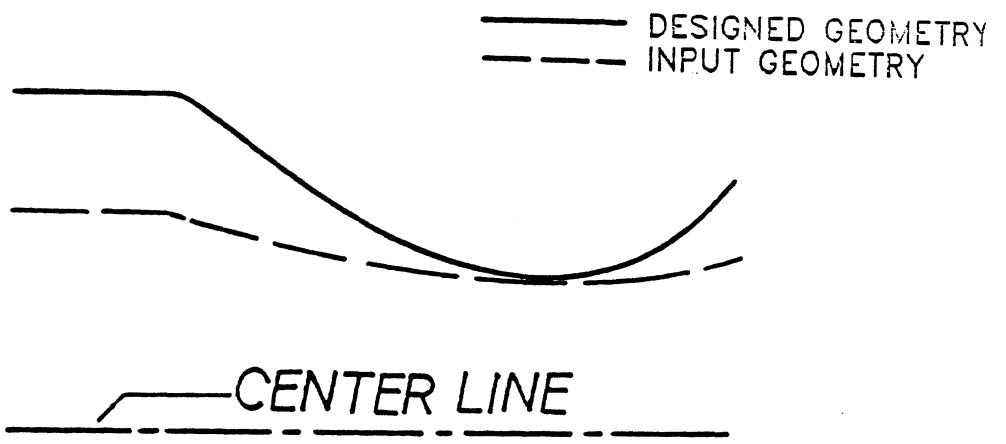

FIG.1.A MODIFICATION OF NOZZLE GEOMETRY

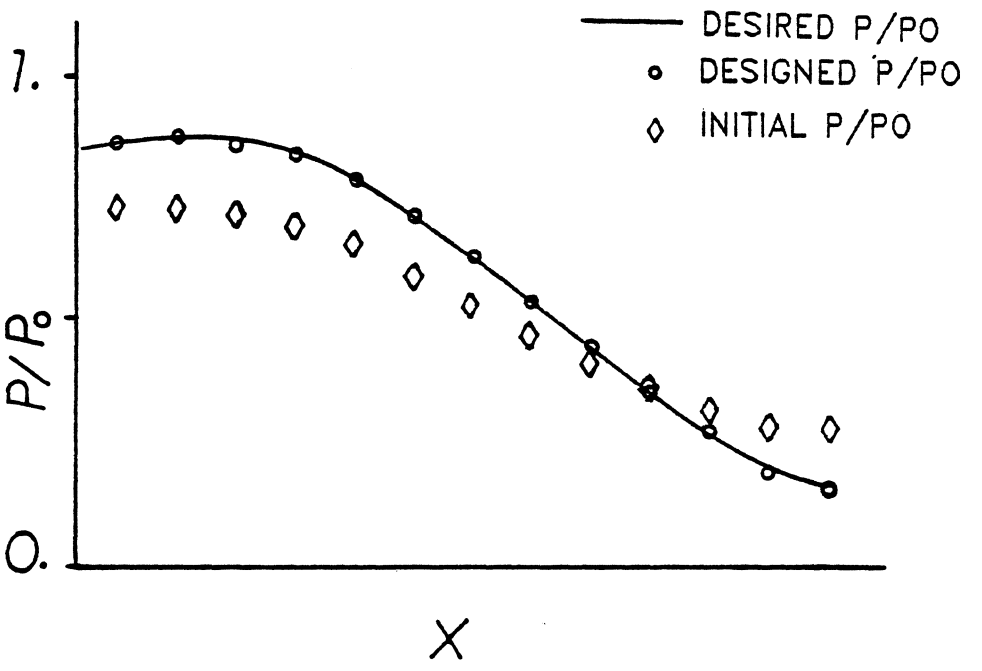

FIG.1.B PRESSURE DISTRIBUTION ON UPPER WALL

1.2 Review of Analysis and Design Methods

The method for computing the wall modification is very similar to the analysis solution with the only differences being in the treatment of the boundary conditions and the specification of the prescribed pressure distribution. Therefore, any method applied to the direct solution of the transonic flow, with some modifications, can be employed for a design calculation.

Two types of the wall boundary conditions are used in the present calculation. They are the Neumann and Dirichlet boundary conditions. If the value of the normal derivative of the dependent variable is prescribed on the boundary, the condition is said to be a Neumann boundary condition. In contrast, if the value of the dependent variable itself is prescribed on the boundary, the condition is known as a Dirichlet boundary condition. In the calculations presented in this thesis, the Neumann boundary condition implies that the surface tangency of the flow is enforced. The Dirichlet boundary condition implies that a pressure distribution is enforced which in turn results in a specified value of the potential function on the boundary. For the Dirichlet boundary conditions, the flow may not be tangent to the surface. Hereafter, the problems with the Neumann and the Dirichlet conditions are referred to as the Neumann and the Dirichlet problems, respectively.

The well-known mathematical difficulties associated with the transonic flows are non-linearity and mixed (elliptic-hyperbolic) nature of the governing equation. Supersonic flows are modeled by hyperbolic

equations and subsonic flows by elliptic equations. A solution to mixed equations is required for a complete description of a transonic flow regime. Murman and Cole (3) in 1970 introduced a finite difference scheme in which the local type of the governing equations is taken into account, and therefore, they overcame the stability problems of the relaxation method. Application of time-dependent and relaxation techniques for direct solutions was discussed by Murman (4). Another major improvement was Jameson's rotated differencing scheme (5) of 1974 in which the equations are locally transformed into a streamline and normal coordinate system. Walsh (6) applied a type-dependent, relaxation method to solve the transonic potential equation in nozzles and good agreement with experimental results was obtained. Brecht (7) further expanded Walsh's method to evaluate the rotational effects by introducing a rotation function to the full potential equation. This allows flows with radial gradients in total pressure to be calculated. Since Brecht's method is used in the present calculation, it is described in more detail in the next chapter.

Tranen (8) and later Henne (9) use an iterative procedure between a direct and indirect calculation for design of airfoils. Tranen starts with an arbitrary airfoil shape and a prescribed pressure or velocity distribution which is integrated to determine the value of potential functions on the starting airfoil surface. Calculation is carried out in a computational plane determined from conformal mapping of the approximate airfoil to a circle. The resulting problem with the Dirichlet boundary condition is then solved by a type-dependent relaxation technique based on the full potential equation. The solution to

the design problem contains the normal velocity component at the surface which is used in a mass conservation equation to determine the position of displaced streamlines. The pressure distribution at the trailing edge is readjusted in order to maintain lift and to assure the satisfaction of the Kutta condition. Then a direct solution over the approximate airfoil shape provides a pressure distribution which is compared with the prescribed pressure distribution. The same procedure is repeated on the new airfoil shape until convergence occurs. Convergence is achieved (if attainable) in the sense that the pressure distribution from a direct solution reaches the desired pressure distribution. The convergence of Tranen's method is not guaranteed because an arbitrarily chosen pressure distribution, and may result in the search for a physically unachievable airfoil shape.

The method developed by Carlson (10) for airfoil design, solves the full potential equation with the mixed (Neumann and Dirichlet) boundary conditions in Cartesian coordinates. In this method the front portion of the airfoil is assumed to be known and a target pressure distribution is prescribed on the remainder of the airfoil surface. To start the design calculation an initial profile for the remaining portion is also needed. The flow field is computed by a relaxation technique. A Neumann boundary condition is applied near the leading edge and a Dirichlet boundary condition is applied over the remainder of the airfoil. The boundary condition near the leading edge is the surface tangency of the flow and for the remainder the target pressure distribution specifies a surface derivative of the potential function in the x direction. Taylor series expansion about the dummy points inside the

boundary are used to express derivatives of the potential function. Two terms in the series are written in finite difference form. Then the resulting equations in conjunction with the equations of boundary conditions in each part of the airfoil are solved for the dummy points inside the boundary. The dummy points are consequently found in terms of the neighboring potentials, slope of the surface, and body position (10) while maintaining the boundary requirements. The solution is relaxed a few cycles and the flow tangency equation is used to find the slope of the surface in the remaining portion of airfoil. The slope is then integrated by a fourth order Runge-Kutta method to find surface ordinates, y. The solution is relaxed again for a few cycles and new ordinates are found until the changes in shape reach a limiting tolerance. Any trailing edge gap is removed by adjusting the input leading edge geometry or pressure.

Volpe (11) in 1983, provided the latest improvement in the inverse design of closed airfoils. He suggested that the prescribed velocity distribution for the airfoil should satisfy three constraints in order to have a solution to the design problem. First, it is required that the speed at infinity have a specified value (usually one), that the angle of attack be specified, and that the trailing edge thickness of the airfoil be specified (11). Closed form expressions for these constraints do not exist for compressible flow. According to Volpe, both Tranen and Carlson ignore the first constraint but consider the trailing edge closure in different ways. Volpe believes disregarding the first constraint causes inconsistency between the design and analysis solutions. He also mentions that the earlier methods developed by

Tranen and Carlson may work without difficulty for small modifications of airfoil geometry, but they fail to converge for larger modifications. In Volpe's method, the constraints are translated into parameters which control the pressure distribution and these parameters are found as part of the solution. A reduced potential function is defined to overcome the singularities introduced by the mapping of airfoil into a circle. Starting with an input profile, the target velocity distribution is integrated on the surface to obtain values of the potential function. The Dirichlet problem for the continuity equation is solved, and a normal component of the velocity on the surface is computed. The flow angle perturbation at the surface is found as the inverse tangent of normal velocity divided by tangential velocity. The airfoil surface is rotated by this angle to become a streamline. The same process is repeated for the new airfoil shape until the changes in flow angle perturbation become negligible and the normal velocity component approaches zero. A detailed description of treatment of constraints in airfoil design can be found in reference 11.

Fortunately, none of the above constraints strictly apply to the case of nozzle design, and any of the described methods with some modifications can be used for the design of propulsion nozzles. A modified Tranen (8) approach together with an analysis method developed by Brown, Brecht, and Walsh (2) are used in the present calculations.

2. METHOD DESCRIPTION

This section describes the inverse method for the design problem of nozzles with transonic pressure distribution. The analysis part of this method was developed by Brecht (7) in 1975. The formulation of the governing equations is taken from his work and only the final equations are described here. Derivation of governing equations and details of coordinate transformation can be found in reference 7. The treatment of boundary conditions for both the analysis and design problems are discussed.

2.1 Governing Equations

In the derivation of the governing equation, a rotation function $F(x,r)$ is introduced, and a velocity function, ϕ, is defined such that

$$\phi_x + F = u$$

$$\phi_r = v$$

where u and v, the axial and the radial components of the velocity, are nondimensionalized with respect to the local stagnation speed of sound, and x and r have been nondimensionalized with respect to the radius of the outer wall at the throat. The rotation function, F, is related to the local vorticity, ω, by the relationship,

$$F_r = \omega$$

where

$$-\omega \equiv \frac{\partial u}{\partial r} - \frac{\partial v}{\partial x} .$$

The rotation function can be related to the radial variation of total pressure, P_o, by Crocco's theorem (12) as

$$F_r = \frac{1}{u\gamma P_o} \left(1 - \frac{\gamma-1}{2} M_o^2\right) \frac{\partial P_o}{\partial r} \tag{2.1}$$

where M_o is the velocity divided by the stagnation speed of sound. Using the velocity function, the non-dimensionalized equation of motion for the steady, axisymmetric, isentropic flow of an ideal gas can then be written as

$$(c^2 - (\phi_r+F)^2)(\phi_{xx}+F) + (c^2 - \phi_r^2)\phi_{rr}^2$$

$$- (\phi_x+F)\phi_r(2\phi_x\phi_r+F_r) + \frac{c^2}{r}\phi_r = 0 \tag{2.2}$$

where c, the local sound speed is given by

$$c^2 = 1 - \frac{\gamma-1}{2}[(\phi_x+F)^2 + \phi_r^2] . \tag{2.3}$$

Equations 2.1, 2.2, and 2.3 are the governing equations used in the calculations.

In order to avoid complicated irregular finite differences at the boundaries of nozzle, a coordinate transformation from the physical plane (x,r) to the computational plane (ξ,ψ) is used. The transformation provides an equally spaced grid system which provides greater computational accuracy than using unequal spacing (13). The transformed equation can be written in the form

$$A\,\phi_{\xi\xi} + B\,\phi_{\xi\psi} + C\,\phi_{\psi\psi} = D \tag{2.4}$$

where

$$A = (c^2 - (\phi_x+F)^2)\xi_x^2$$

$$B = 2\,(c^2 - (\phi_x+F)^2)\,\xi_x\psi_x - 2\,(\phi_x+F)\,\phi_r\xi_x\psi_r$$

$$C = (c^2 - (\phi_x+F)^2)\,\psi_x^2 + (c^2-\phi_r^2)\,\psi_r^2$$

$$- 2\,(\phi_r+F)\,\phi_r\psi_x\psi_r$$

$$D = (\phi_x+F)\,\phi_r F_r - \frac{c^2}{r}\,\phi_r - (c^2-(\phi_x+F)^2)(F_x+\phi_\psi\psi_{xx}) \tag{2.5}$$

$$+ 2(\phi_x+F)\,\phi_r\phi_\psi\psi_{xr}.$$

The transformed equations are solved by numerical relaxation using Jameson's (5) rotated differencing scheme.

The analysis and design calculations utilize exactly the same governing equations, coordinate transformation, and finite difference approximations. The only difference between the two schemes is the treatment of the boundary conditions along the wall. In both the design and analysis methods, the calculation is stopped when the maximum change in Mach number is less than a specified value, usually 0.001.

2.2 Boundary conditions

In both design and analysis calculations, a constant area inlet section is added to the nozzle. At the beginning of this inlet, the potential function is set equal to a constant which means the radial velocity is zero. The exit conditions consist of a prescribed potential function for subsonic exit flow. For supersonic exit flow no exit boundary conditions are prescribed. If the calculations are to contain the rotational effects, the total pressure is specified as a function of radius at the inlet.

The wall boundary conditions will be described for the design and analysis calculations individually in the next sections.

2.2.1 Wall Boundary Conditions - Analysis Calculations

For the analysis calculations a Neumann boundary condition on the velocity function, ϕ, which enforces flow tangency at the wall and centerline is applied. Because of the parabolic nature of Eq. 2.1 for the rotation function, F, only a condition in the inner wall (or centerline) is needed. In Brecht's analysis calculations two different specifications of F are possible. In one case, F is set to zero along the inner wall or centerline, and in the other case, the values of F are

set equal to the local axial velocity components. In the present calculations the former boundary condition on F is used.

2.2.2 Wall Boundary Condition - Design Calculations

For the design calculations a Dirichlet boundary condition is applied on the wall to be modified and a Neumann condition is applied on the other wall. To provide the Dirichlet condition, the prescribed pressure distribution is first translated to a velocity distribution by means of one-dimensional gas dynamic theory to give

$$M_o = \left[\frac{2}{\gamma - 1} \left[1 - \left(\frac{P}{P_o}\right)^{\frac{\gamma-1}{\gamma}} \right] \right]^{1/2} \qquad (2.6)$$

where M_o is the velocity divided by the stagnation speed of sound. Since the flow is tangent to the surface,

$$\phi_s = M_o$$

where s is the streamline coordinate and ϕ is the velocity function.

In the computational plane ϕ_s can be written as

$$\phi_s = \phi_\xi \xi_s + \phi_\psi \psi_s$$

where ξ_s and ψ_s are geometrical (metric) derivatives of ξ and ψ. But along solid boundaries the ψ lines do not change and a wall represents a line of constant ψ. As one marches along the stream direction, at the wall, no changes of ψ are observed. Thus, along the wall,

$$\psi_s = 0$$

and

$$\phi_s = \phi_\xi \xi_s \quad .$$

Application of the chain rule yields

$$\xi_s = \xi_x x_s + \xi_r r_s$$

in which x_s and r_s can be found from the geometry as

$$x_s = \cos \theta$$

$$r_s = \sin \theta$$

where θ is the wall angle measured from the x axis. It should be noted that θ is the actual wall angle and since the flow tangency condition is not enforced the flow angle is expected to be different from the wall angle. Since $\xi = \xi(x)$ *is not a function of r, then $\xi_r = 0$ and therefore ϕ_s or M_o can be written as

$$M_o = \phi_\xi \xi_s = \phi_\xi \xi_x \cos \theta \tag{2.7}$$

Using a centered finite difference for ϕ_ξ,

---

*This is part of the coordinate transformation which is discussed in detail in Reference 7.

$$\phi_\xi = \frac{\phi_{i+1,j} - \phi_{i-1,j}}{2\Delta\xi}$$

allow the velocity function on the surface to be found from

$$\phi_{i+1,jmax} = \phi_{i-1,jmax} + \left(\frac{M_{o\ i,jmax}}{\xi_x \cos\theta}\right)(2\ \Delta\xi) \qquad \text{(outer wall)}$$

$$\phi_{i+1,0} = \phi_{i-1,0} + \left(\frac{M_{o\ i,0}}{\xi_x \cos\theta}\right)(2\Delta\xi)\ . \qquad \text{(inner wall)}$$

In order to prevent uncoupling of the odd and even numbered axial stations, the velocities at the mid grid points are found. Now a forward difference is used for ϕ_ξ. Then ϕ 's are found by marching from the nozzle entrance where the values of ϕ are assumed to be zero using one of these equations,

$$\phi_{i+1,jmax} = \phi_{i,jmax} + \left(\frac{M_{o\ i+1/2,jmax}}{\xi_x \cos\theta}\right)\Delta\xi \qquad \text{(outer wall)} \qquad (2.8a)$$

$$\phi_{i+1,0} = \phi_{i,0} + \left(\frac{M_{o\ i+1/2,0}}{\xi_x \cos\theta}\right)\Delta\xi\ . \qquad \text{(inner wall)} \qquad (2.8b)$$

The boundary condition on the unmodified wall is a Neumann condition.

The use of equations 2.8a and 2.8b implies that F must be zero along the Dirichlet boundary. Now, since for rotational flow calculations (that is for flows which contain radial pressure gradients) Brecht's calculations allow a zero value of F to be enforced along the inner wall only, only the inner wall can be modified if rotational effects are present.

3. DESIGN PROCEDURE

Using the initial wall geometry and the desired pressure distribution, the Dirichlet conditions are determined along the wall in question and the design calculations carried out. When the relaxation cycles end, a normal velocity component is expected to exist on the wall because in the Dirichlet problem the condition that the flow be tangent to the wall is not enforced. The normal velocity component on the wall is found by using the fact that $V_n = \phi_n$. In the computational plane ϕ_n can be written as

$$\phi_n = \phi_\xi \xi_n + \phi_\psi \psi_n$$

where ϕ_ξ and ϕ_ψ are found by the finite difference approximations. In the case of ϕ_ψ a one-sided second-order-accurate finite difference expression is used. In the case of ϕ_ξ a centered (also second-order-accurate) finite difference expression is used. ξ_n and ψ_n, are the geometrical derivatives of ξ and ψ, and are found by the following relations. Application of the chain rule yields

$$\xi_n = \xi_x x_n + \xi_r r_n$$

$$\psi_n = \psi_x x_n + \psi_r r_n$$

in which x_n and r_n can be found from the geometry as

$$x_n = -\sin\theta$$

$$r_n = \cos\theta$$

where θ is the wall angle (see section 2.2.2). Hence, the design solution contains normal velocities at the wall, as shown (by the component $V_{n_{i-1/2}}$) in Fig. 2, which can be found by the above procedure. A mass flux balance is used to calculate the displacement of the streamlines. This results in the equation

$$\rho_i V_{s_i} \delta_i - \rho_{i-1} V_{s_{i-1}} \delta_{i-1} = \left[\frac{\rho_i V_{n_i} + \rho_{i-1} V_{n_{i-1}}}{2}\right] \Delta S \qquad (3.1)$$

where ρ is the density, V_s is the tangential velocity, V_n is the normal velocity, δ is the displacement of the streamline, and ΔS is the arc length on which the balance is made. Dividing Eq. 3.1 by ρ_o, the stagnation density, and rearrangement gives displacement as

$$\delta_i = \frac{1}{\frac{\rho_i}{\rho_o} V_{s_i}} \left[\frac{\rho_{i-1}}{\rho_o} V_{s_{i-1}} \delta_{i-1} + \left(\frac{\frac{\rho_i}{\rho_o} V_{n_i} + \frac{\rho_{i-1}}{\rho_o} V_{n_{i-1}}}{2}\right) \Delta S\right] \qquad (3.2)$$

where $\frac{\rho}{\rho_o}$ is found from the prescribed pressure ratio, $\frac{P}{P_o}$, by one-dimensional isentropic relations. To calculate displacement δ for all points on the wall a starting value must be known. It is the user's choice to indicate where the known displacement is taken. (For example, in the case of designing the upper wall of the hyperbolic nozzle test

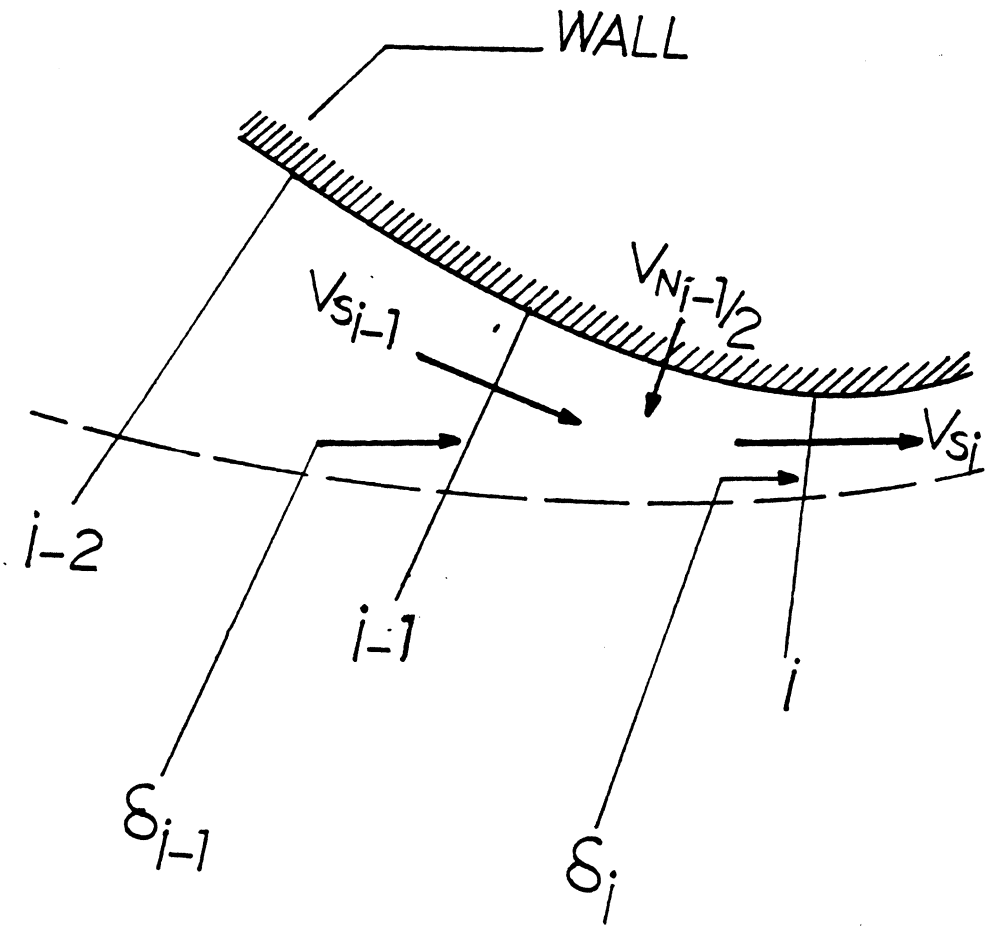

FIG.2 MASS FLUX CONTROL VOLUME

cases, the displacement at the throat is assumed to be zero and displacements on two sides of the throat are calculated using Eq. 3.2). Once the displacements are found, they are either under or over-relaxed by a factor which has to be determined by experience. The following equations are used for under and over-relaxation,

$$\delta_i' = (1-\Omega 1)\ \delta_i \tag{3.3a}$$

$$\delta_i' = (1+\Omega 2)\ \delta_i \tag{3.3b}$$

where $\Omega 1$ is the under-relaxation factor, $\Omega 2$ is the over-relaxation factor, and prime indicates the new values of δ. The proper selection of these factors is needed to insure the convergence of the calculations. The important effects of these factors are shown by plots and discussed in detail in the next chapter. After relaxing the values of displacements, the new wall radii can then be obtained which describe the new nozzle shape.

As mentioned in previous sections, analysis and design calculations are combined together to provide a complete inverse method to design a nozzle. A flow chart is provided in the Appendix to show in detail how these calculations are combined.

The calculations begin with a specification of the initial geometry and the desired pressure distribution. The one-dimensional theory of gas dynamics is used to obtain an initial solution. The problem (with Neumann boundary condition) is then solved by a relaxation process. Once an analysis solution for the input geometry is obtained, the pres-

sure distribution is compared with the desired one. If the comparison is unfavorable, a design calculation is initiated. The design problem (with Dirichlet boundary conditions) is then solved by a relaxation process. As a result of these calculations, normal velocities at the surface to be modified are found, and the geometry of the nozzle is modified accordingly. A new initial solution for the second analysis calculations is obtained by retrieving the previous analysis solution. The results of the second analysis solution reveal whether the new profile provides the desired pressure distribution. Modifications of the wall are repeated in this fashion until the calculated pressure distribution from the analysis solution agrees with the desired one. Convergence is assumed when the minimum difference between the calculated and the desired pressure ratio at each computational point along the designed wall is less than 0.007. In some cases, it has been observed that even though the desired wall pressure distribution has not been reached, very small adjustments in the wall geometry result from the calculations. In fact, the modifications of the wall become so small that an analysis solution of the new geometry does not provide any significant changes in pressure distribution compared to the previous analysis solution. Hence, if the maximum displacement of the wall is less than 0.2% of the average radius then the calculations are stopped. This check avoids useless expenditure of computer time.

4. RESULTS

The inverse method described in the preceding sections is coded in Fortran IV for an IBM 3081 computer. A WATFIV compiler is used for the calculations.(The Fortran H extended compiler is three times faster than the WATFIV compiler.) Cases with various prescribed pressure distributions are tested which include design of hyperbolic and typical turbofan bypass nozzles. A 25 x 11 grid system was used for calculations of the hyperbolic nozzle, and since the turbofan bypass nozzle calculations require much larger computational time, a 13 x 6 grid system was used to save on computer time. Unless specifically mentioned, all test cases presented below have converged to within the 0.007 limit on pressure ratio described in the previous section. The cases where the calculations were stopped due to small wall displacements are specially noted. Design of the wall of axisymmetric hyperbolic nozzles will be considered first.

4.1 Hyperbolic Nozzle Test Cases

The shape of the hyperbolic nozzle is given by

$$R_o = [1+Bx^2]^{1/2}$$

where R_o , the wall radius, and x , the distance measured from the throat, are nondimensionalized with respect to the radius of the outer wall at the throat, and B is the reciprocal of the radius of curvature of the nozzle at the throat. In order to construct test cases Brecht's (7) program was run for three hyperbolic nozzles having a B value of

0.1, 0.15, and 0.20. Hereafter, these geometries are noted by symbols N1, N2, and N3 and for future reference, this nomenclature is shown in Table I. Table II summarizes the test cases described in this section.

For the first case, the N2 geometry was input along with the pressure distribution of the N1 geometry (see Table I) obtained from Brecht's (analysis) program. It is expected here that the N1 geometry will result from these calculations. As Carlson (10) indicates, this numerical consistency between the analysis and design calculations is necessary to prove the validity and consistency of the inverse method. Convergence in this case was achieved in two modifications of wall geometry. A total CPU time of 216 seconds was used. In Fig. 3, three different pressure distributions are shown plotted against axial station number where the axial station number is the axial coordinate index. The first pressure distribution which is shown by a solid line corresponds to the desired pressure distribution which in this case is the pressure distribution obtained from the N1 geometry. The second pressure distribution shown by diamond symbols corresponds to the input (N2) geometry. The third pressure distribution is shown by the circle symbols and corresponds to the final pressure distribution obtained by the design calculations. As can be seen the designed pressure distribution is indistinguishable from the desired one. In Fig. 4 the geometry corresponding to the input nozzle shape is shown by dashed lines and the final nozzle geometry corresponding to the desired pressure distribution is shown by triangles. The solid line corresponds to the N1 geometry. As can be seen the final nozzle geometry is indistinguishable from the N1 geometry. This excellent agreement demonstrates the numerical consistency of this design technique.

TABLE I

NOZZLES GEOMETRIES

No.	Wall	Centerbody
N1	Hyperbolic (B=0.10)	No
N2	Hyperbolic (B=0.15)	No
N3	Hyperbolic (B=0.20)	No
N4	Hyperbolic (B=0.10)	Yes (R_i=0.3)
N5	See Fig. 18	Yes
N6	See Fig. 18	Yes

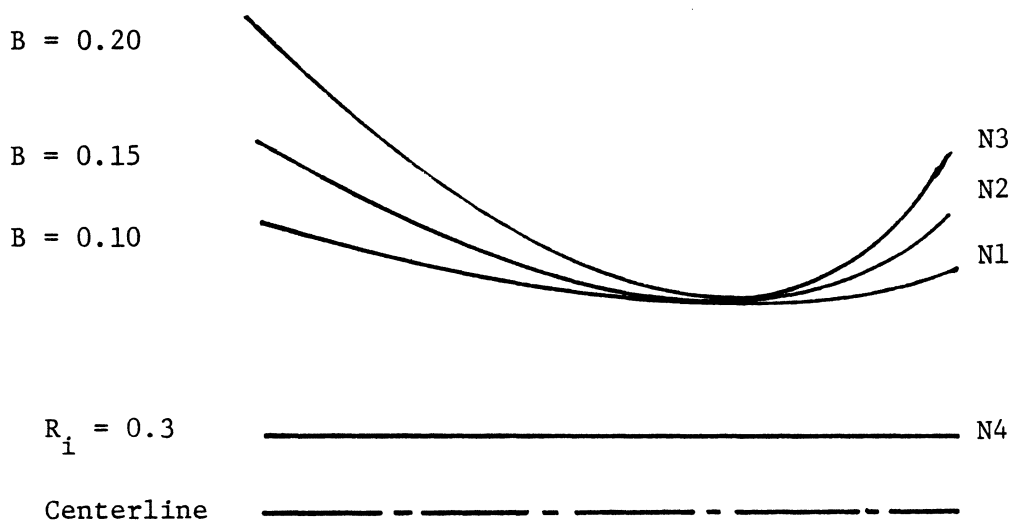

TABLE II

SUMMARY OF TEST CASES

TEST CASE	MESH	BOUNDARY MODIFIED	INPUT GEOMETRY	PRESSURE DISTRIBUTION	INLET CONDITION	NO. OF DESIGN CALC.	COMPUTATION TIME(SEC)
1	25x11	Wall	N2	N1	Uniform	2	216
2	25x11	Wall	N3	N1	Uniform	3	291
3	25x11	Wall	N1	N2	Uniform	3	268
4	25x11	Wall	N1	N3	Uniform	3	266
5	25x11	Centerbody	N1	N4	Uniform	2	297
6	25x11	Centerbody	N1	N4	Nonuniform	3	390
7	13x6	Centerbody	N5	N6	Uniform	5	84
8	13x6	Centerbody	N5	N6	Nonuniform	7	68

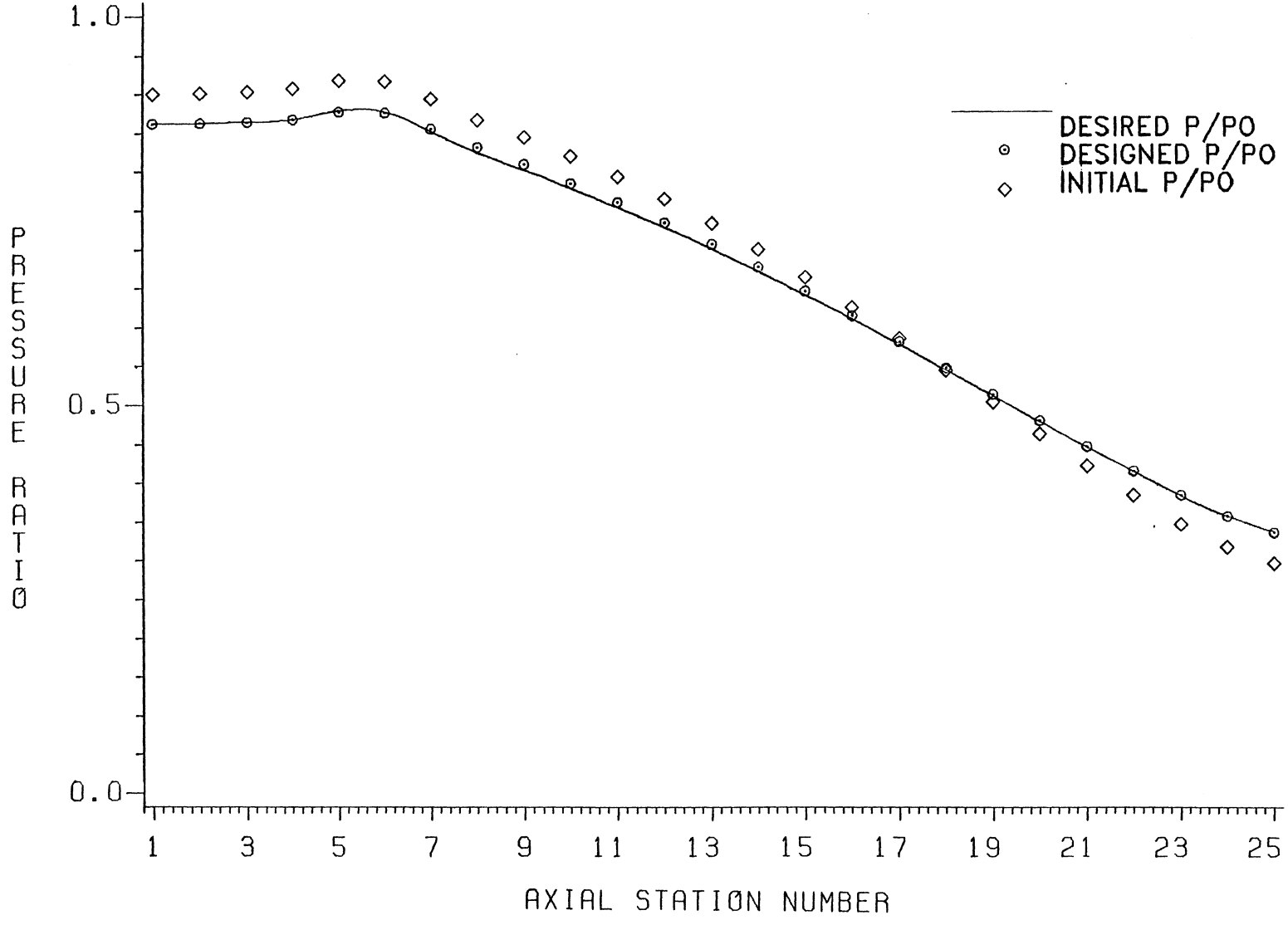

FIG.3. OUTER WALL PRESSURE DISTRIBUTION OF HYPERBOLIC NOZZLE (CASE 1)

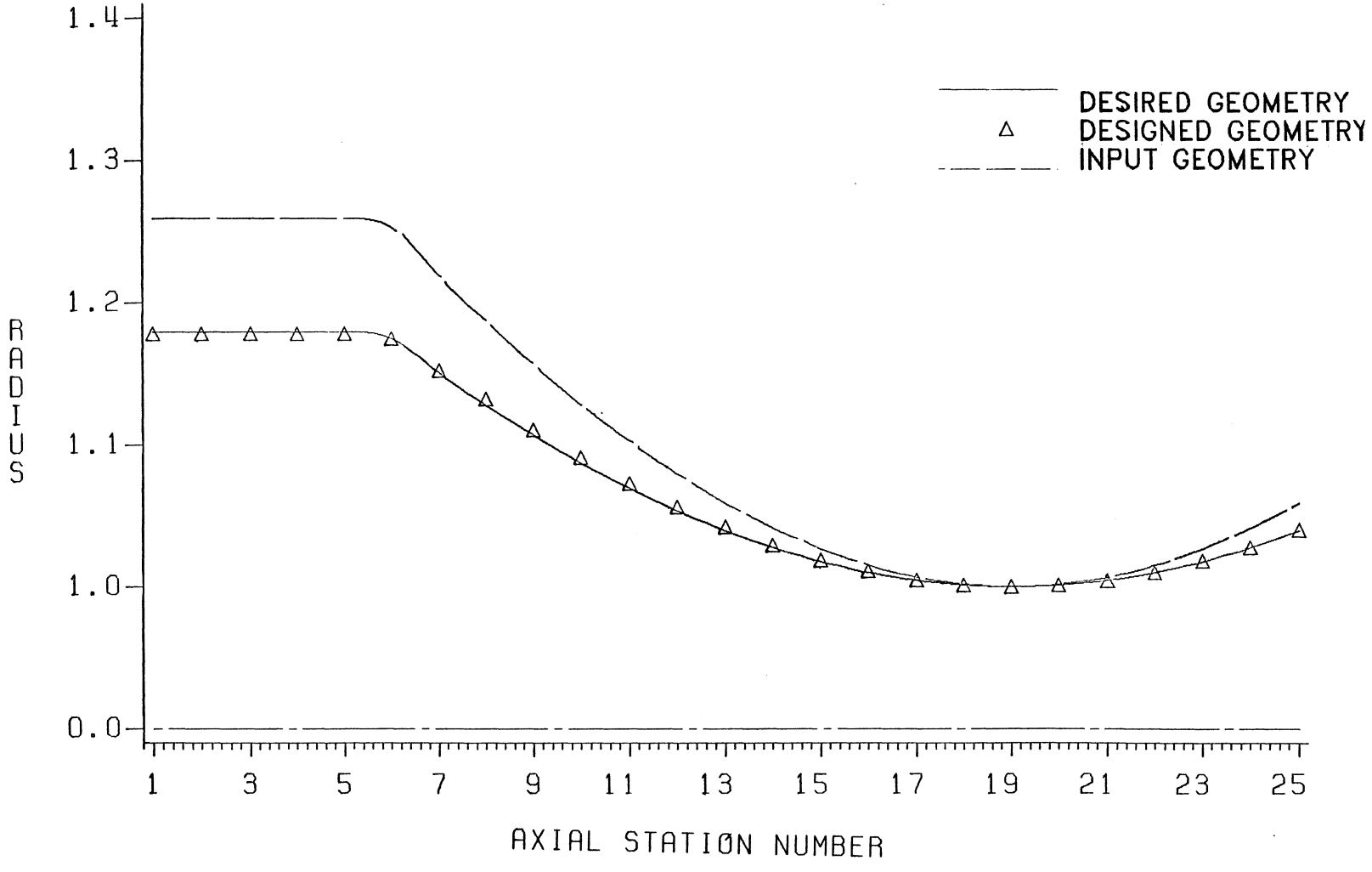

FIG.4. OUTER WALL DESIGN OF HYPERBOLIC NOZZLE (CASE 1)

In order to test the ability of the inverse method to make a more severe modification of the nozzle wall geometry, a second test was run using N3 and N1 geometry which is shown in Table II. Namely, the N3 geometry was the initial guess for a nozzle which was to be designed with a pressure distribution corresponding to the N1 nozzle. As can be seen from Fig. 5, the differences between the initial and the desired pressure distributions is about double that for the first test case. However, once again a pressure distribution indistinguishable from the desired one was obtained. As can be seen in Fig. 6, geometrical adjustments in the nozzle geometry were more than double that required in the first test case, but again excellent agreement with the anticipated results was obtained. In this case, three design calculations using a total CPU time of 291 seconds were completed before the final geometry was obtained.

The preceding two test cases resulted in making the channel narrower. In order to demonstrate the ability of the program to design a channel which was wider than the initial guess, the role of the initial and desired conditions were reversed in the next two cases. As shown in Table II, test case three consists of an input geometry of N1 and a pressure distribution corresponding to N2 geometry. Figures 7 and 8 show the results of the third test case which converged after three design calculations and used 268 seconds of CPU time. The figures reveal the excellent agreement of the final pressure distribution (corresponding to the designed geometry) with the desired pressure distribution of the N2 geometry. The designed geometry is almost identical to the N2 geometry. Again, in order to test the inverse method for an even

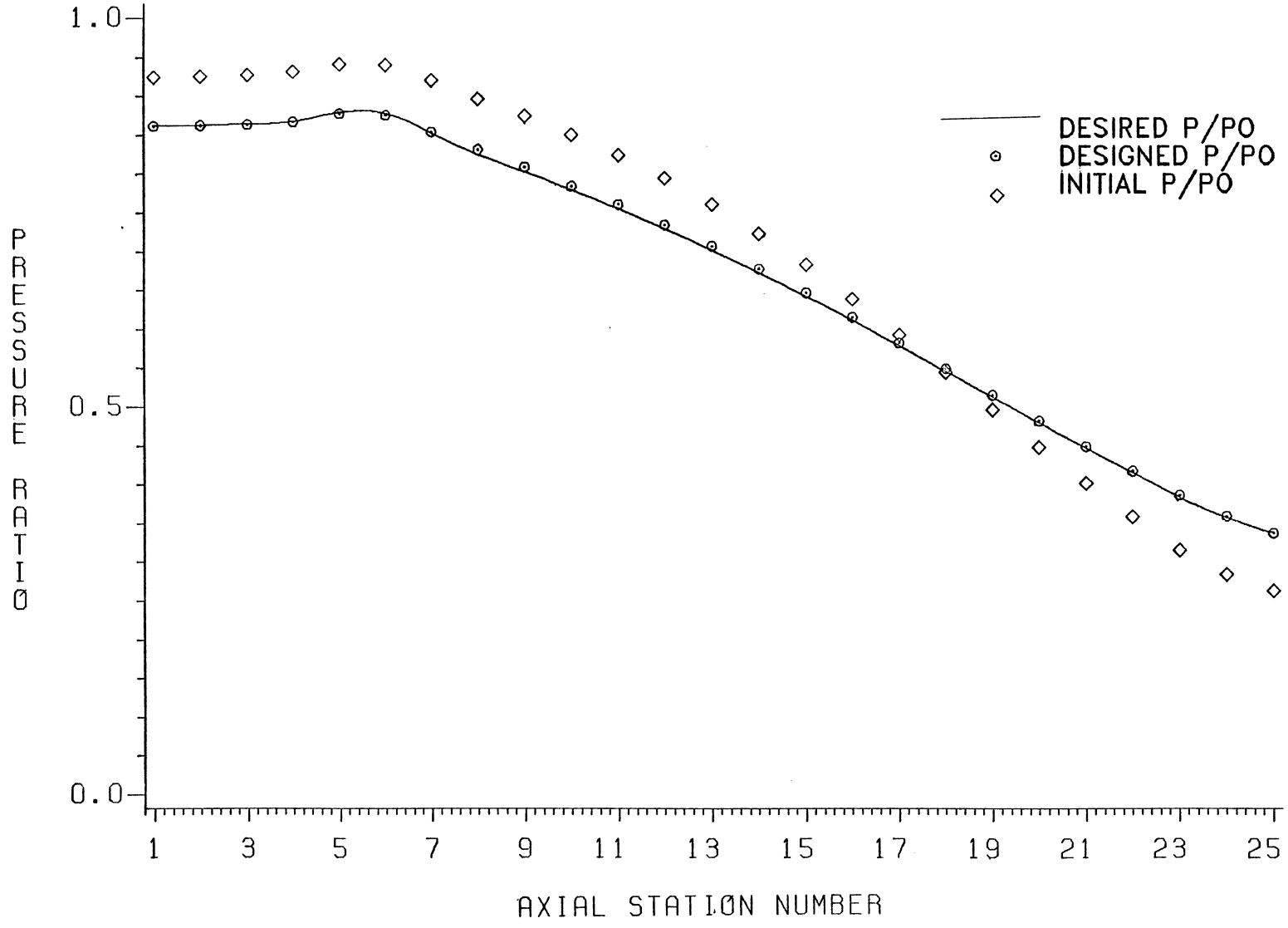

FIG.5. OUTER WALL PRESSURE DISTRIBUTION OF HYPERBOLIC NOZZLE (CASE 2)

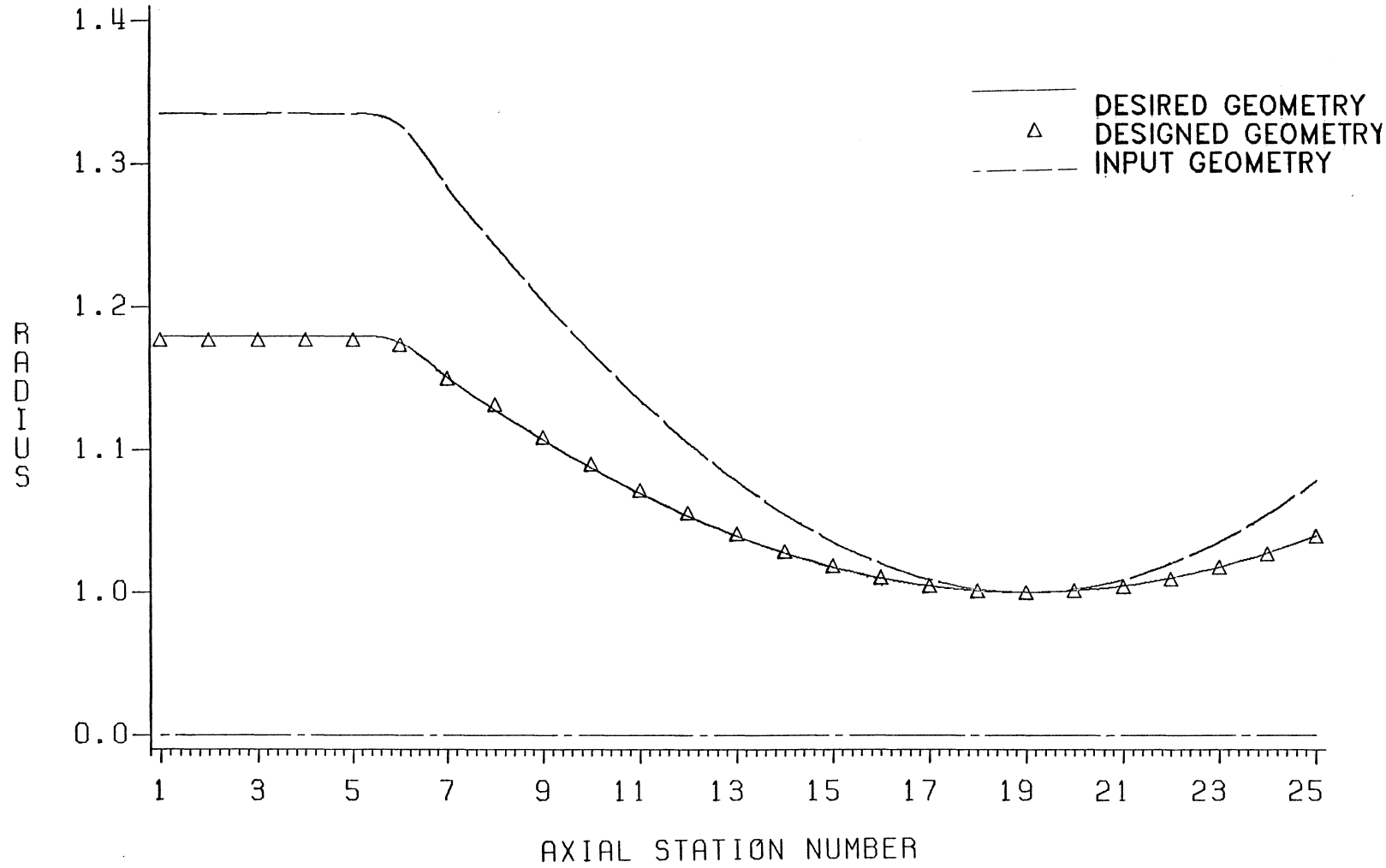

FIG.6. OUTER WALL DESIGN OF HYPERBOLIC NOZZLE (CASE 2)

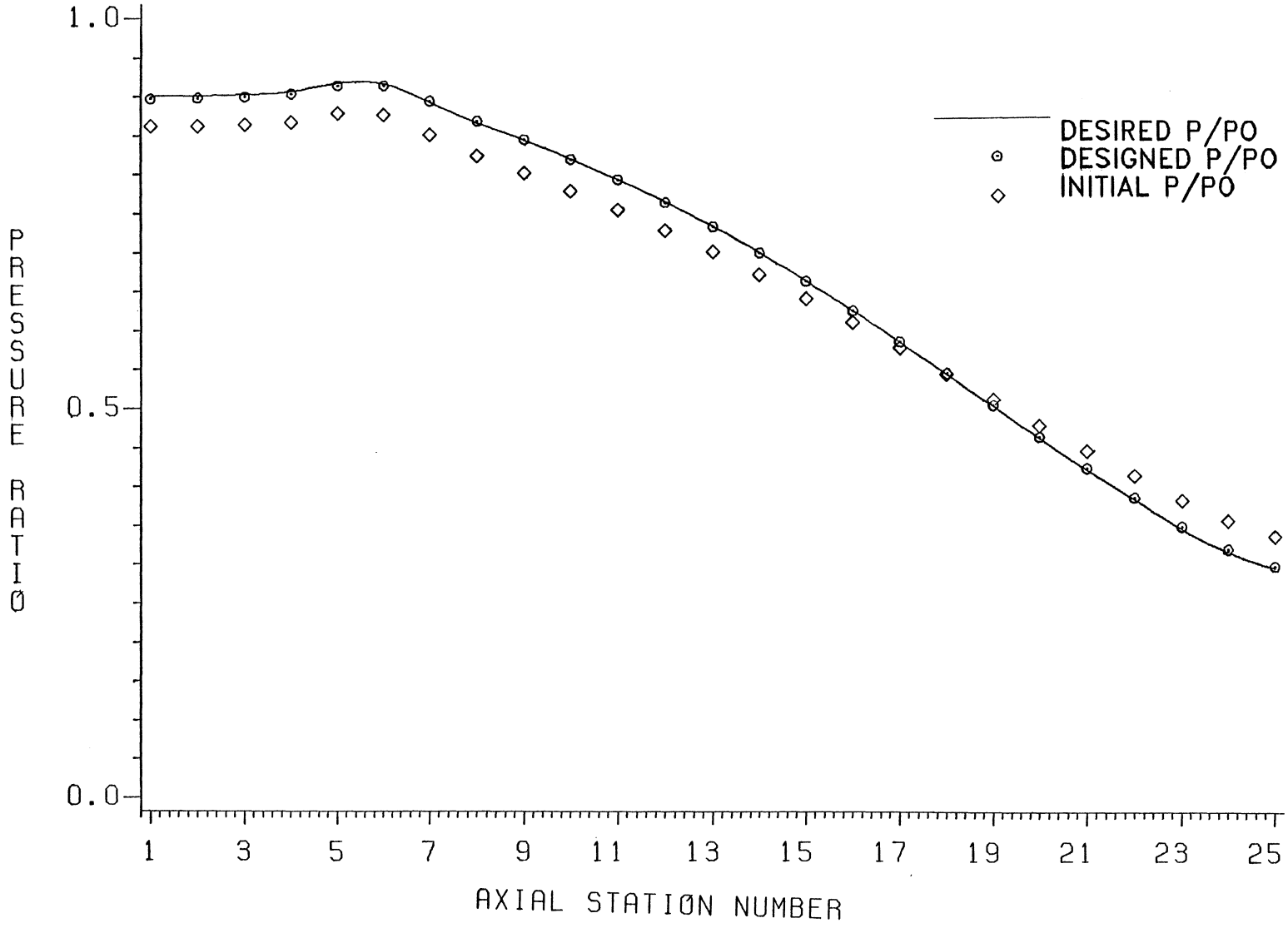

FIG.7. OUTER WALL PRESSURE DISTRIBUTION OF HYPERBOLIC NOZZLE (CASE 3)

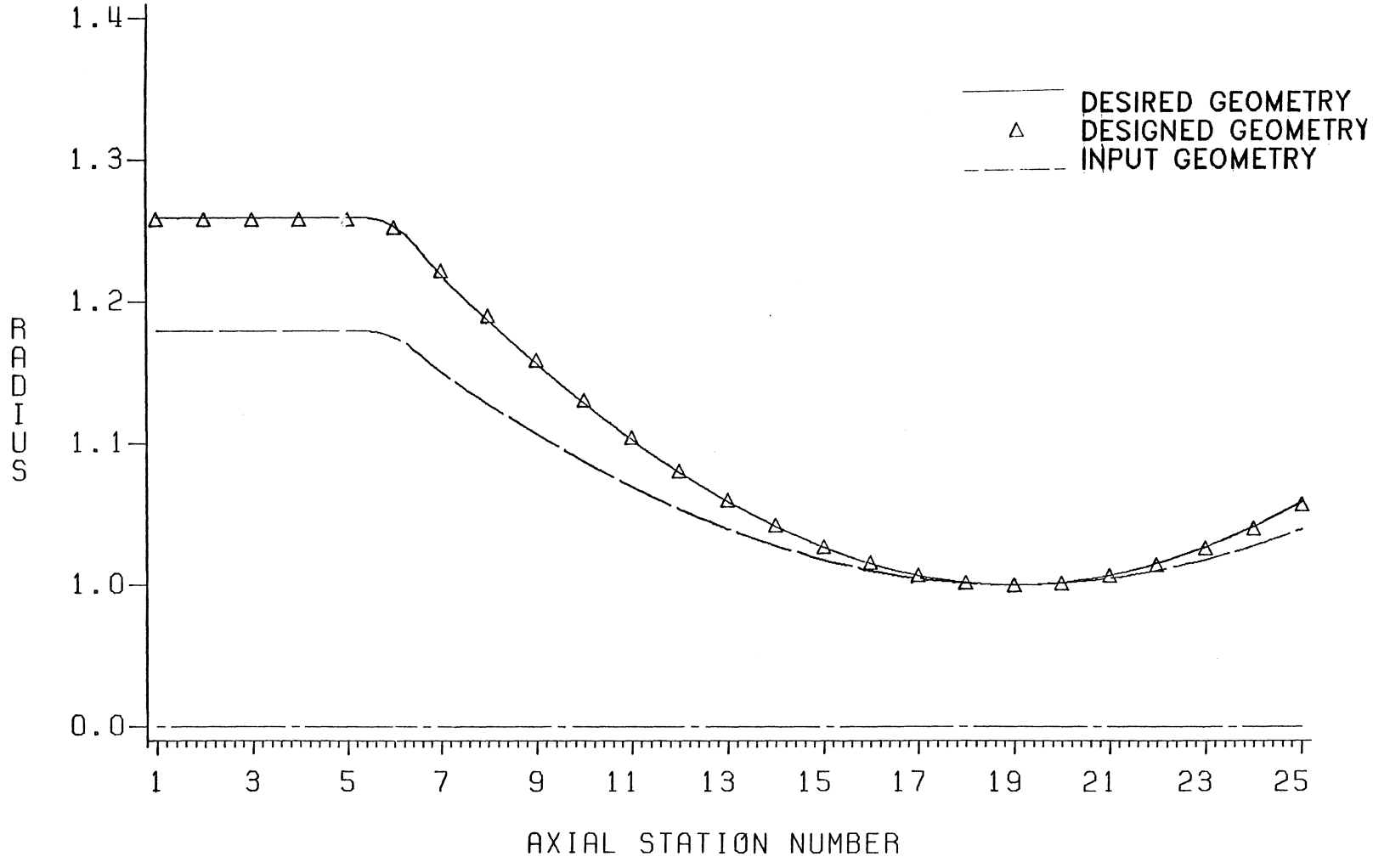

FIG.8. OUTER WALL DESIGN OF HYPERBOLIC NOZZLE (CASE 3)

more severe widening of the nozzle wall, a fourth test case was run in which a N1 input geometry and the pressure distribution of the N3 geometry were used. The results are plotted in Figs. 9 and 10 in which the same symbols as before are used to distinguish the input, desired, and designed conditions. Although the modifications were double that required in the third test case, once again the resulting pressure distribution was almost identical to the desired one and the designed geometry was indistinguishable from the expected N3 geometry. This calculation converged, and the N3 nozzle geometry was obtained after three design calculations which used 266 seconds of CPU time. It should be mentioned that in the above test cases the outer wall radius at the throat was kept constant. Therefore, an initial zero displacement at the throat was specified.

In carrying out the above test cases, the need for under or over-relaxing the values of displacements after each design calculation was discovered. The selection of a proper under-relaxation factor, $\Omega 1$, or over-relaxation factor, $\Omega 2$, was essential in successful completion of the design procedure. In some cases an optimum geometry may never be found if an unappropriate displacement relaxation factor is used. For the first two cases, an under-relaxation factor of 0.3 was used which provided the most efficient design calculation for these cases. For the third test case, an over-relaxation of 0.10 and for the fourth test case a value of zero was used. In order to investigate the effect of under or over-relaxation factor, test case three was once more run using an under-relaxation factor of 0.40. Test case three did not converge for this value. Since the final desired shape was known in advance, check-

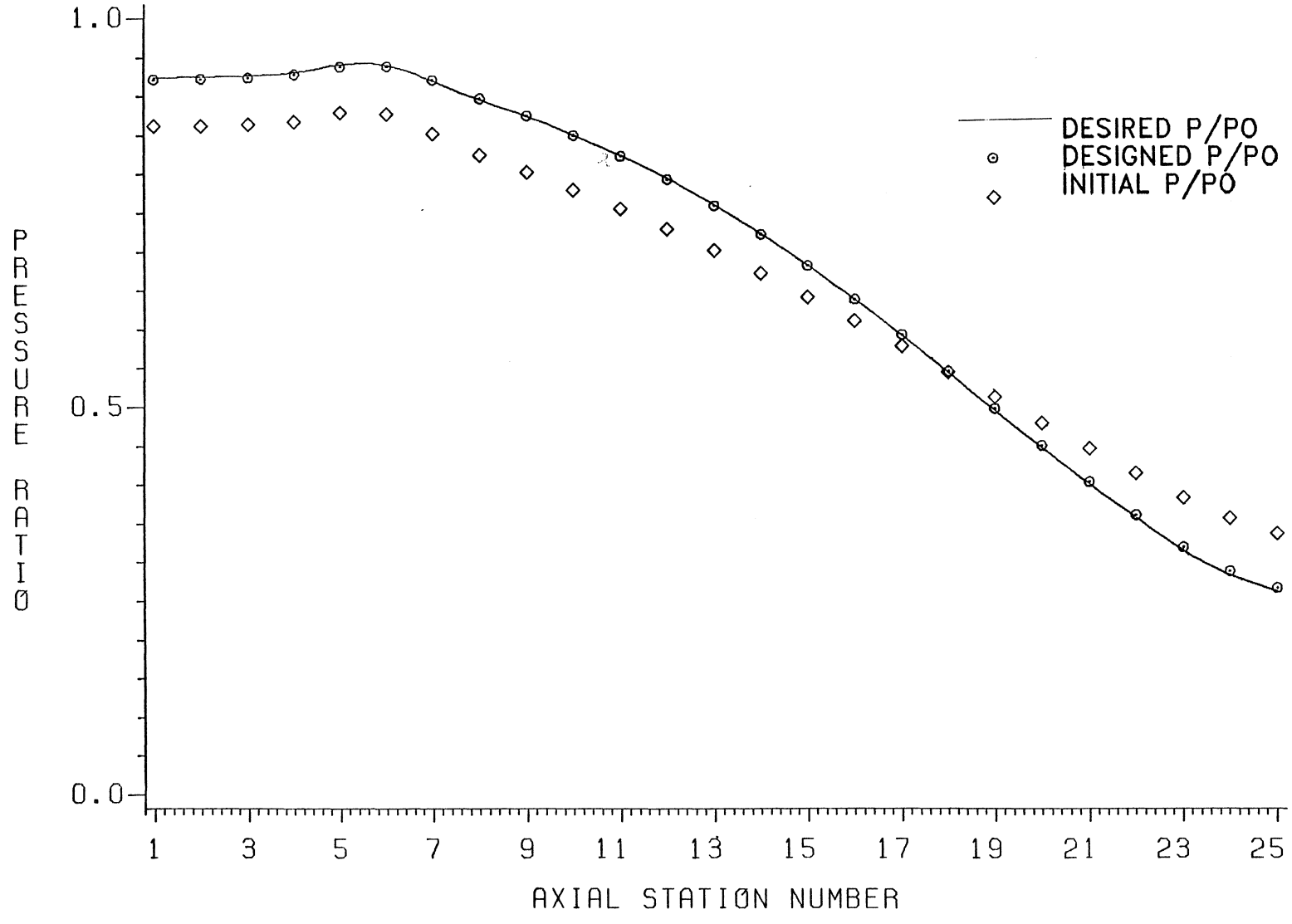

FIG.9. OUTER WALL PRESSURE DISTRIBUTION OF HYPERBOLIC NOZZLE (CASE 4)

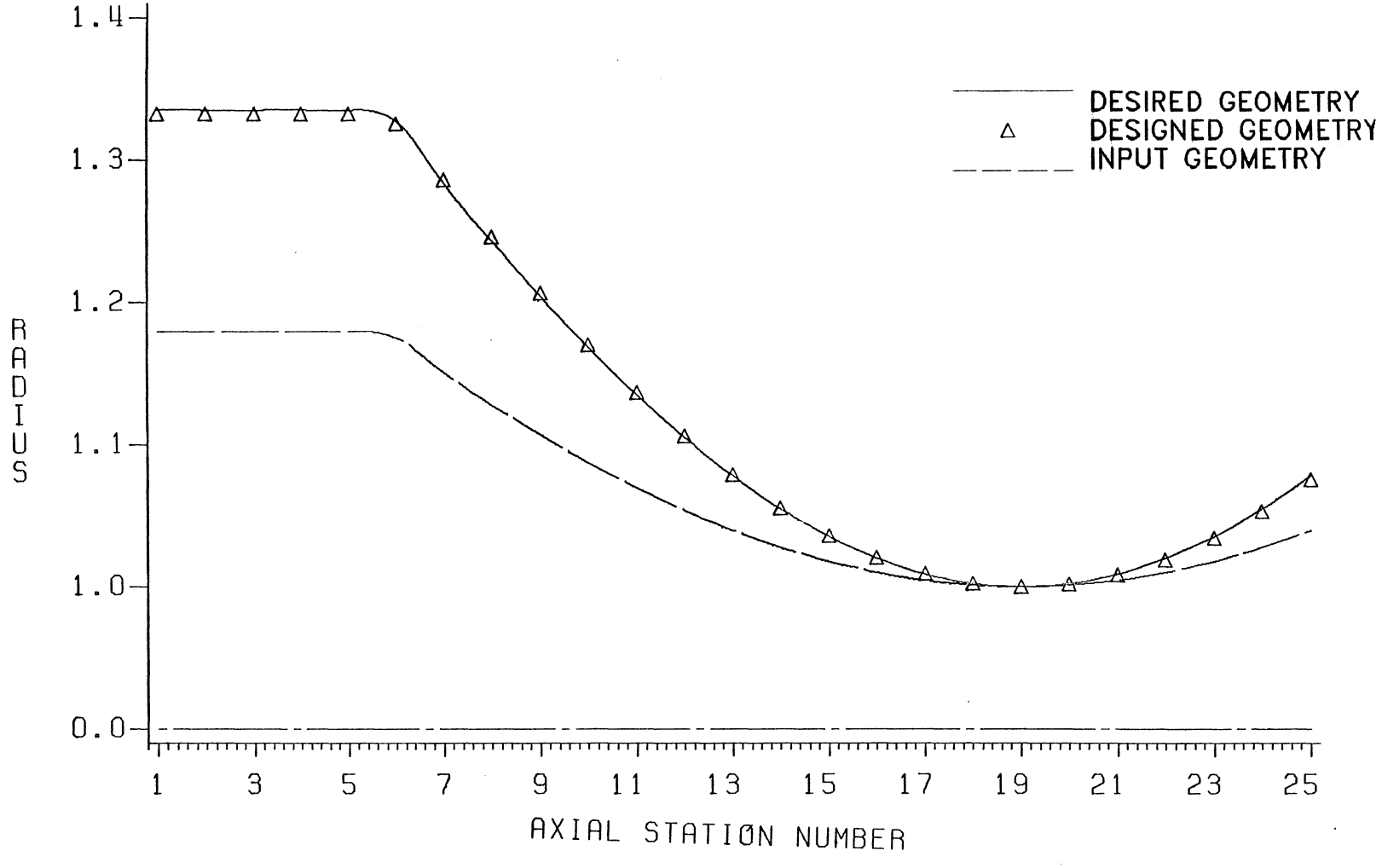

FIG.10. OUTER WALL DESIGN OF HYPERBOLIC NOZZLE (CASE 4)

ing the calculated displacements after each design calculation could show how far they are from the desired displacements. Using an under-relaxation of 0.40 for test case three caused a smaller modification in geometry than what was expected after each design calculation. Consequently, the optimum shape was never reached. However, as mentioned earlier in this section, in order to achieve a converged result, it was necessary to over-relax the displacements and a value of 0.10 was found to be satisfactory. It is interesting to trace the "dynamics" of the wall adjustments produced by using the 0.10 over-relaxation factor. The first wall modifictions (of the three required for convergence) were larger than the modification needed to reach the optimum geometry, and they resulted in a nozzle shape which was even wider than the desired shape. This over-shooting was caused by application of an over-relaxation factor. However, in the second design calculations, some negative displacements were calculated which compensated for the previous over-shoot, and finally, the third design calculation provided the nozzle shape which produced the desired pressure distribution. Figures 11 and 12 show the changes in wall radii for successive design calculations for relaxation factors of $\Omega 1 = 0.40$ and $\Omega 2 = 0.10$ respectively. The oscillation of displacements caused by application of the 0.10 over-relaxation factor can be clearly seen in Fig. 11. In these two figures the number chains represent the displacements produced at the iteration having that number. Further comments on selection of the displacement relaxation factors is provided in Section 4.3.

In the fifth test case the ability of the calculations to adjust the geometry of the inner wall (centerbody) of a hyperbolic nozzle was

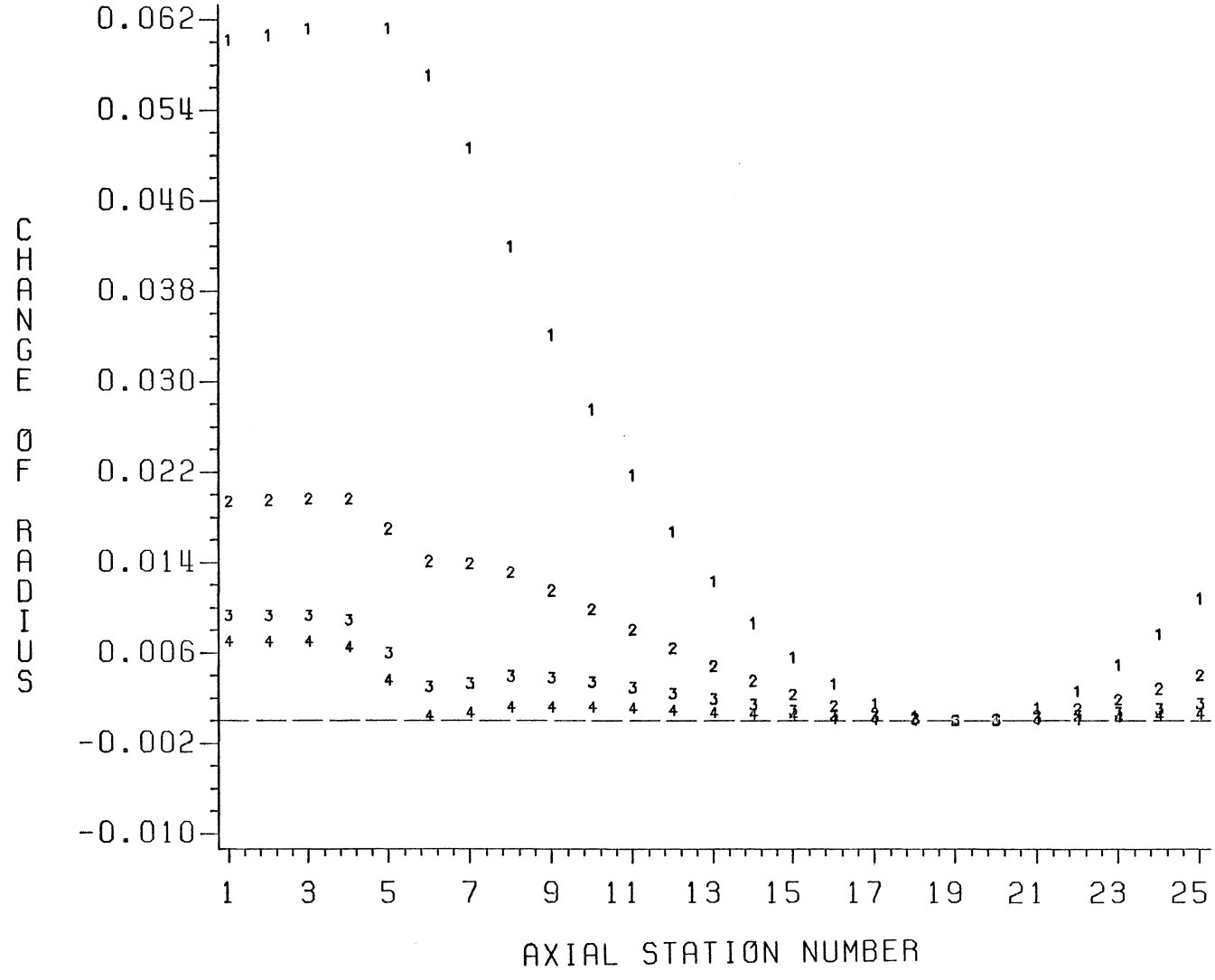

FIG.11. WALL RADIUS DISPLACEMENT (CASE 3, $\Omega 1=0.40$)

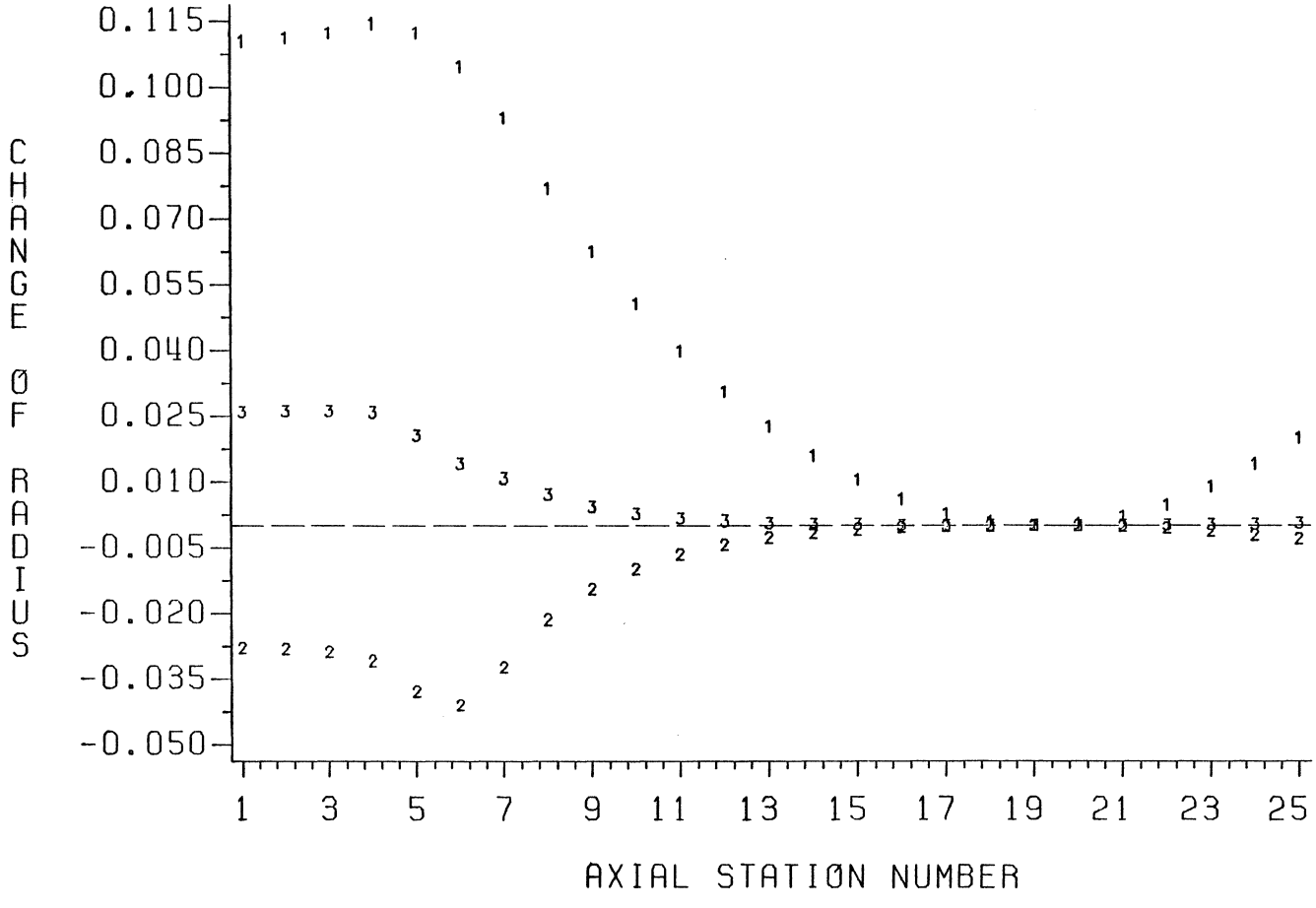

FIG.12. WALL RADIUS DISPLACEMENT (CASE 3, $\Omega 2=0.10$)

investigated. This test case involved a nozzle of fixed outer wall geometry and a pressure distribution which corresponds to a geometry with a cylindrical centerbody. The input pressure distribution corresponds to the N4 geometry (see Table II). The N4 geometry (see Table I) is a hyperbolic nozzle with a radius of curvature equal to that of N1 geometry with a cylindrical centerbody of radius 0.3. In these calculations a value of zero was used for the (under/over) relaxation factor. The calculation of wall displacement was begun at the inlet station where the inner wall displacement corresponding to the radius of the N4 centerbody was specified. The calculated pressure distribution converged to the desired one after two design calculations using a total CPU time of 297 seconds. Figure 13 shows the excellent agreement of the designed (final) pressure distribution with the desired one corresponding to N4 geometry, and Fig. 14 shows that the calculated centerbody is indistinguishable from the N4 centerbody. When this test case was run with specified wall displacement at the inlet rather than at the throat, the run was unsuccessful and convergence was not obtained. Observing the calculated displacements revealed that very small values were found in the inlet region. However, reasonable values of displacement were calculated downstream of the throat. No special reason for failure of this case could be deduced from the observations.

None of the above cases involved the rotational flow effects. A sixth test case which included such effects was run to check the ability of the inverse method to design nozzles with radial pressure gradients. As indicated in section 2.2.2, for such cases only the centerbody can be modified. The input geometry corresponded to the N1

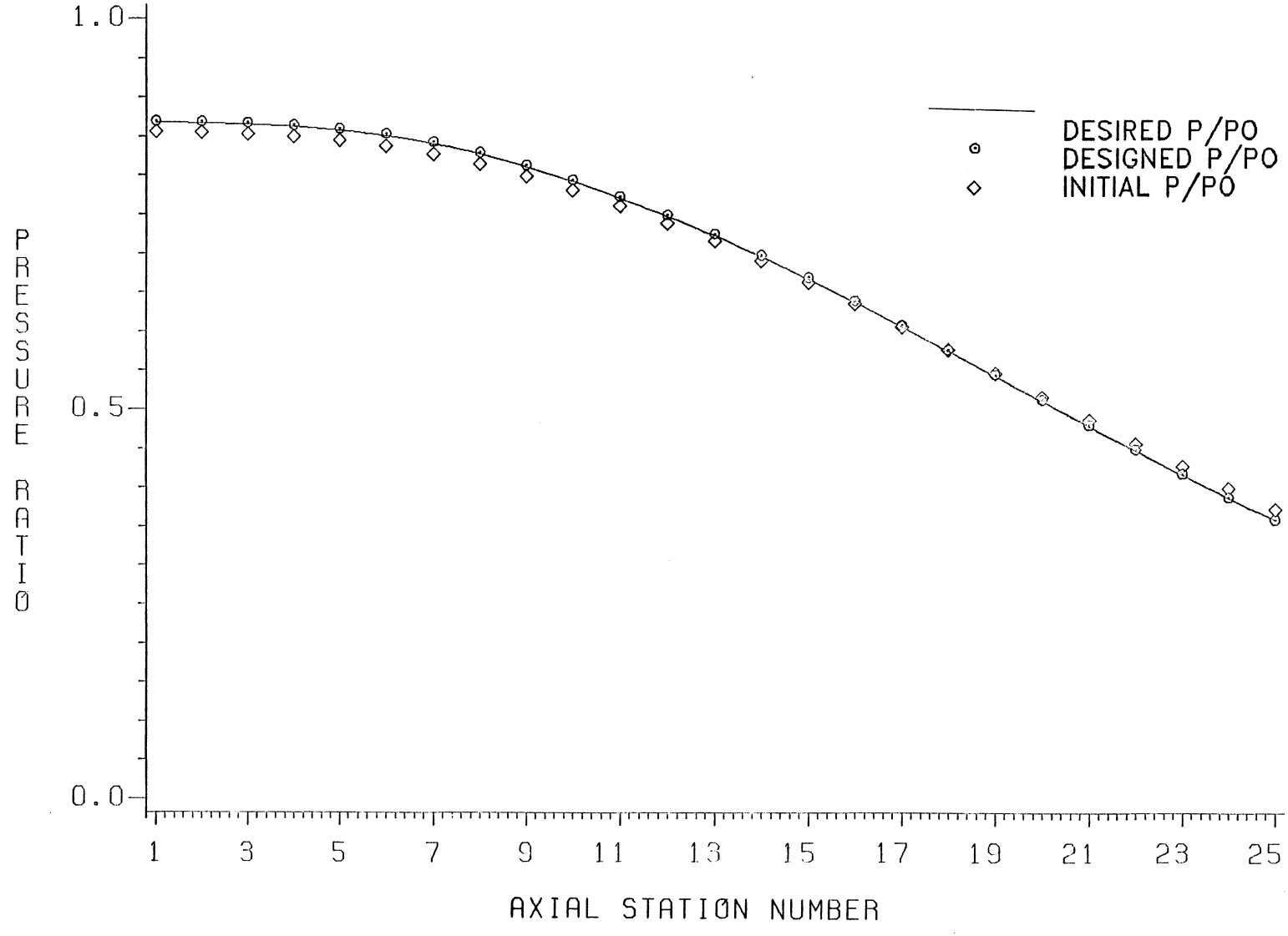

FIG.13.CENTERBODY PRESSURE DISTRIBUTION OF HYPERBOLIC NOZZLE (CASE 5)

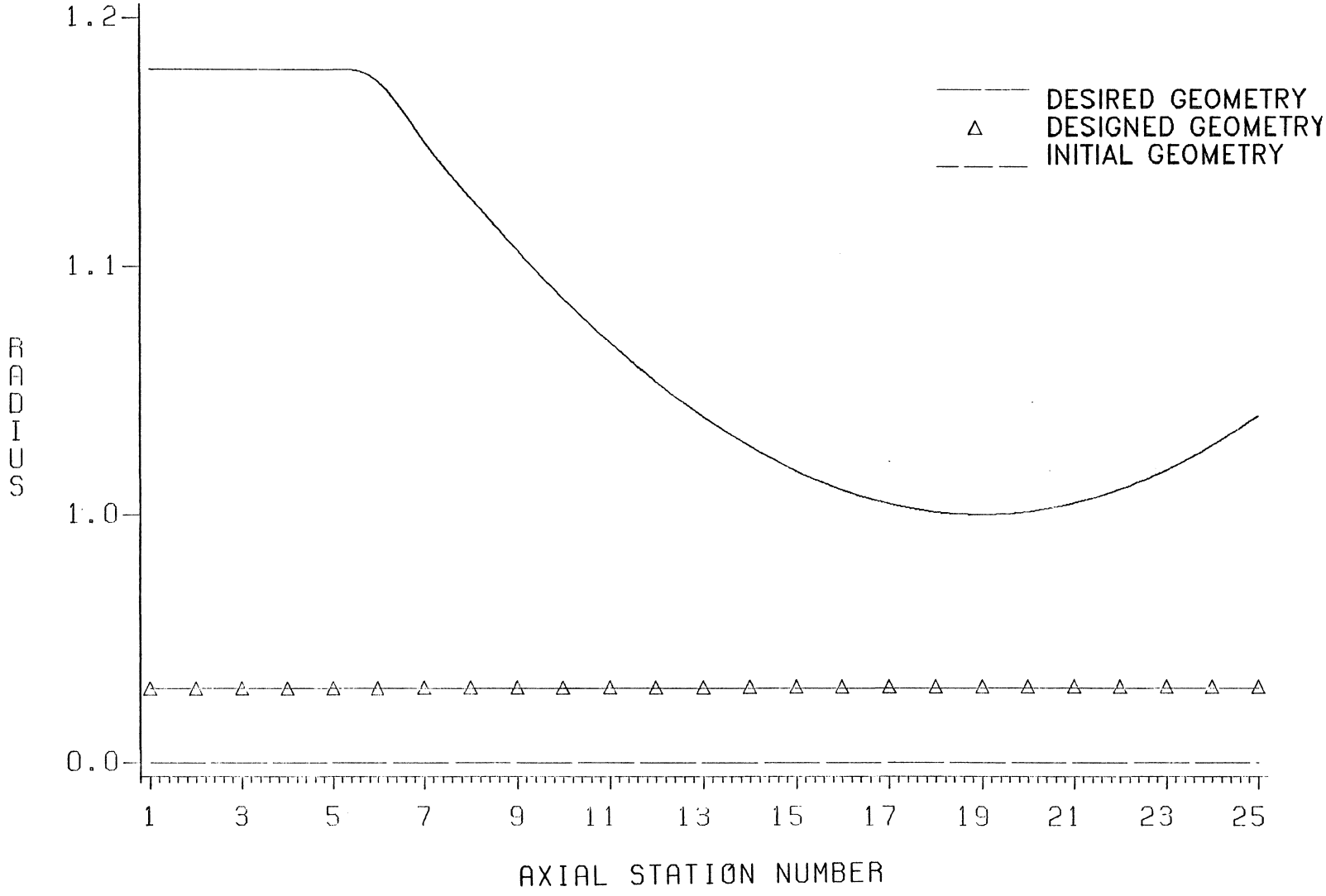

FIG.14. CENTERBODY DESIGN OF HYPERBOLIC NOZZLE (CASE 5)

shape. For rotational flow calculations, the radial variation of total pressure at the inlet must be supplied. The total pressure profile used is shown in Fig. 15. The desired pressure distribution corresponded to the N4 geometry with the inlet total pressure profile shown in Fig. 15. For this case a value of zero for displacement relaxation factor was used. The displacement corresponding to the centerbody of radius was supplied just as in test case five except that the displacement was specified at the throat rather than at the inlet. The pressure distribution converged to the desired one after completion of three design calculations utilizing a total CPU time of 390 seconds. This test case was completed successfully and the designed geometry was identical to N4 geometry. Figures 16 and 17 show the excellent agreement between desired and designed conditions.

4.2 Turbofan Bypass Nozzle Test Cases

The previous test cases utilized a geometry which had an analytical shape. Test case seven was run in order to check the abilities of the program to modify the geometry of a duct which is described in pointwise coordinate pairs. The duct chosen was a CF6-50 fan bypass duct used in Brecht's 1975 paper. Another bypass duct geometry with the same outer wall as the above duct but with a different inner wall configuration is also considered for this test case. These two geometries are shown in Fig. 18 and they are denoted as N5 and N6 respectively in Table I. Note in Fig. 18 the radial coordinate (unlike previous plots) is dimensional. The dimension of the radial coordinate is in inches.

The N5 geometry was input along with the pressure distribution corresponding to the inner wall of the N6 geometry. As described

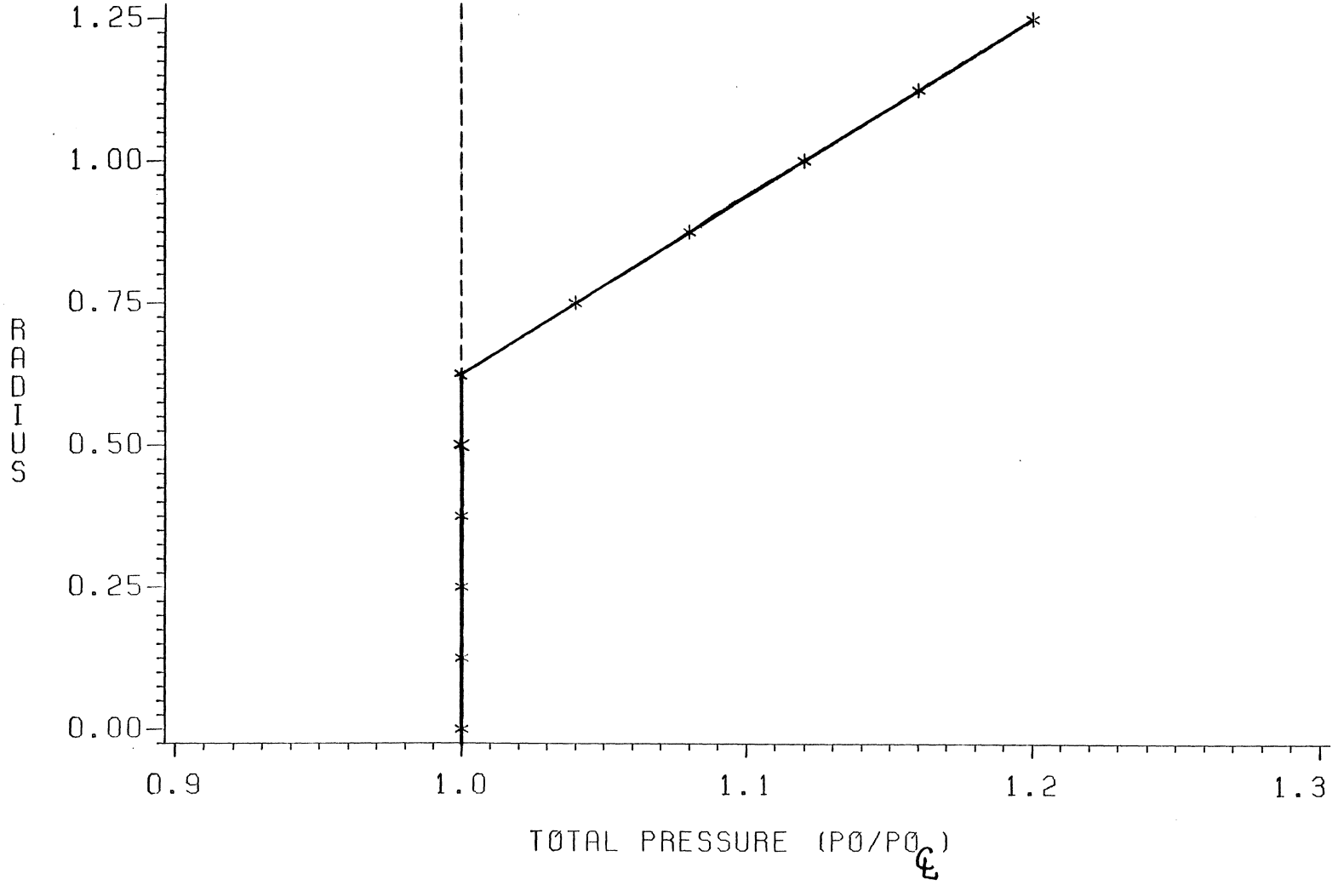

FIG.15. INLET TOTAL PRESSURE VARIATION (CASE 6)

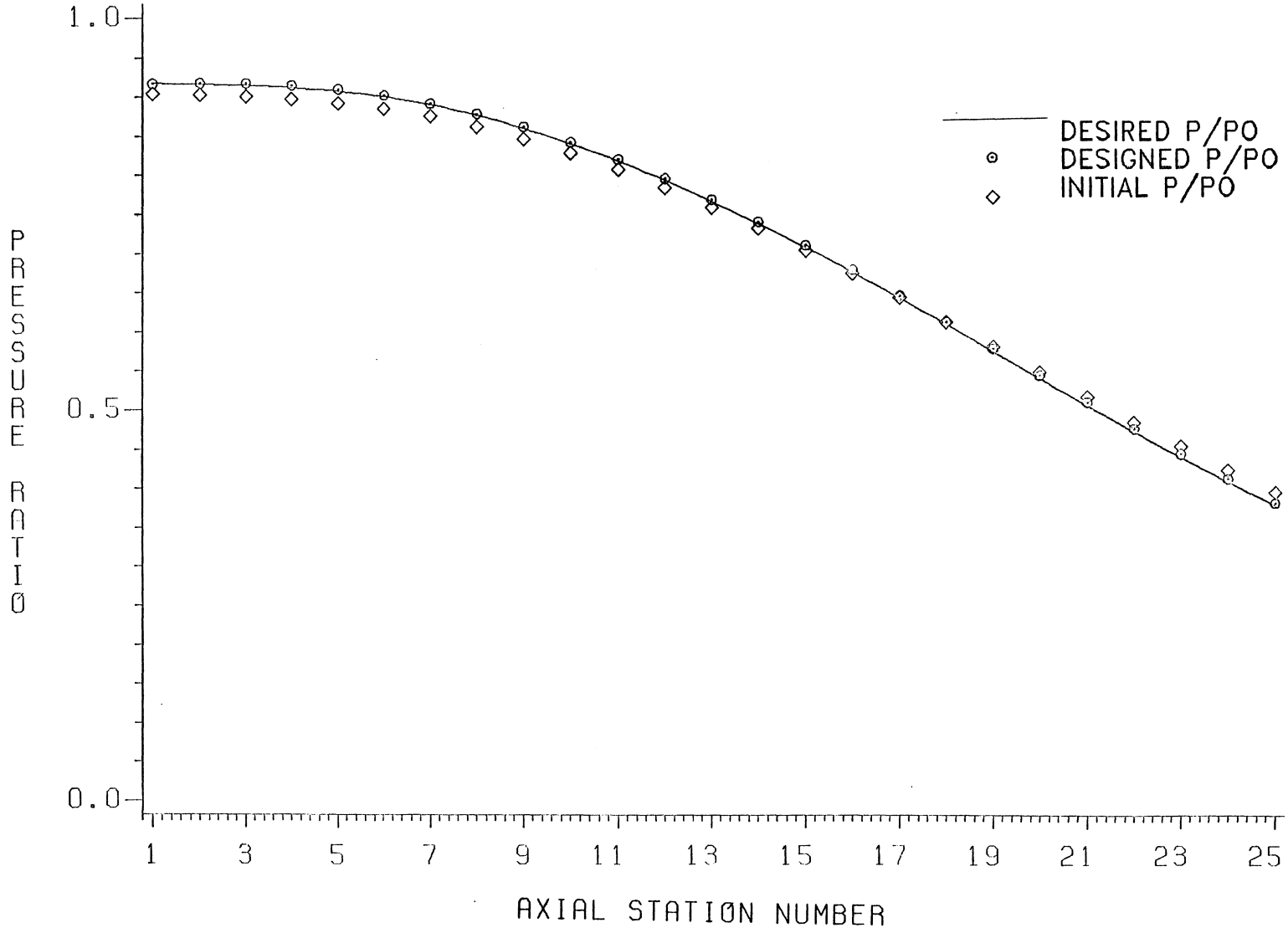

FIG.16.CENTERBODY PRESSURE DISTRIBUTION OF HYPERBOLIC NOZZLE (CASE 6)

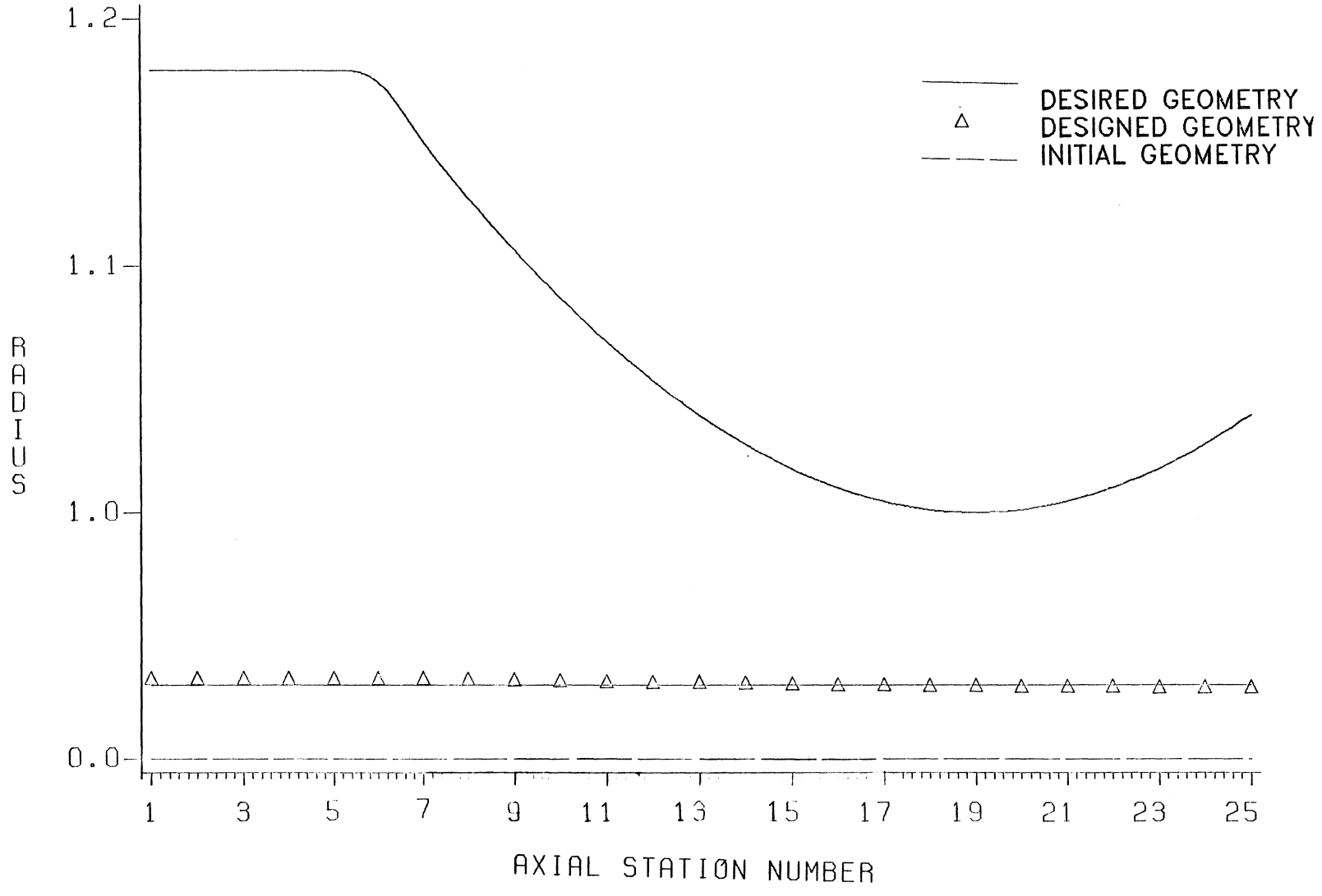

FIG.17. CENTERBODY DESIGN OF HYPERBOLIC NOZZLE (CASE 6)

earlier in this chapter, utilizing a 25 x 11 grid system for calculations on these duct geometries proved to be very time consuming. Therefore, an reduced grid system of 13 x 6 mesh points was used to reduce computational time. This test case was run with a displacement underrelaxation factor of 0.2. The calculations of displacements began at the throat where a zero value of displacement was specified. The convergence of the pressure distribution was not obtained in this case. However, the calculation was stopped after five design calculations in accordance with the procedure described in Chapter 3. This calculation used 84 seconds of CPU time. Although the convergence of pressure distribution was not obtained,the results as shown in Fig. 19 indicated a calculated pressure distribution almost indistinguishable from the desired one. The nozzle geometry in Fig. 20 is also quite close to N6 geometry.

In order to check the ability of the inverse method to design bypass ducts with rotational flow effects, the eighth and final test was run with a N5 input geometry including the input total pressure profile shown in Fig. 21. The desired pressure distribution for this case corresponded to N6 geometry with the same total pressure profile. Although the computational time for these calculations was reduced by increasing the grid spacing, the reduction was not sufficient when the rotational flow effects were included in the calculations since more than 1500 iterations were required before convergence of the analysis calculation was achieved. Such large number of nozzle iterations could enormously increase the computational time required for the inverse method. Therefore, to further reduce the cost, the Mach number conver-

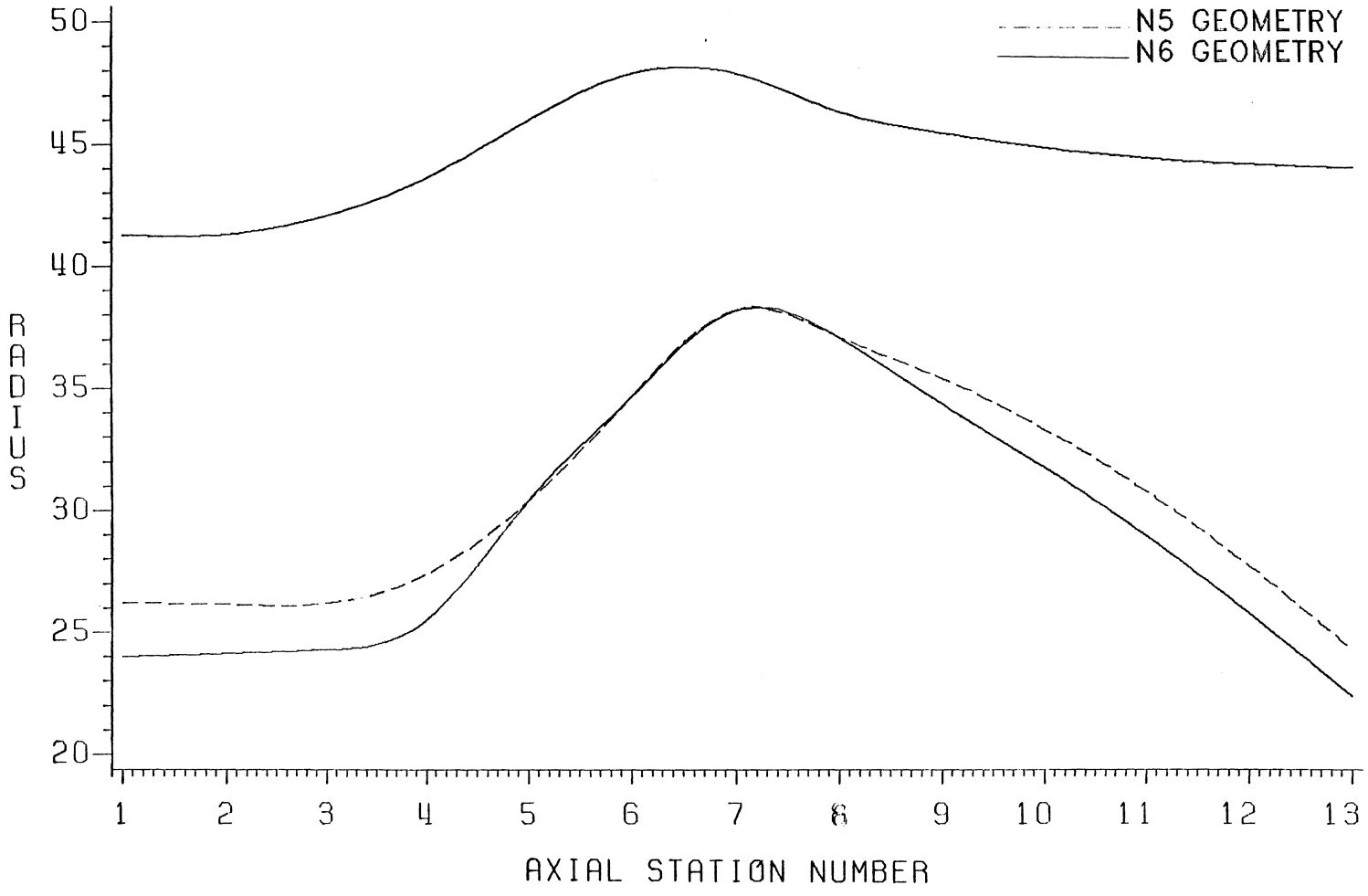

FIG.18. TURBOFAN BYPASS DUCT GEOMETRY

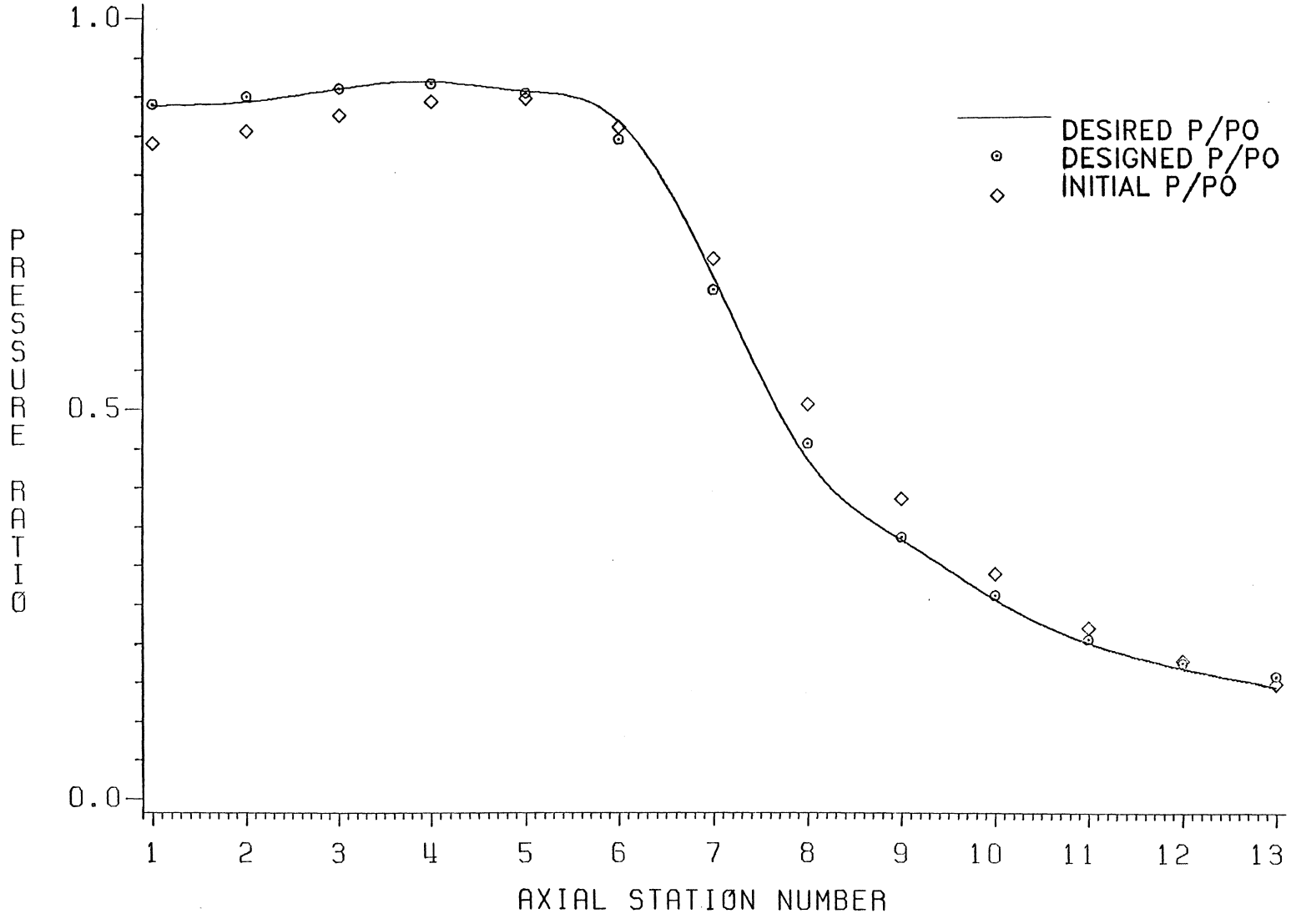

FIG.19. INNER WALL PRESSURE DISTRIBUTION OF BYPASS DUCT (CASE 7)

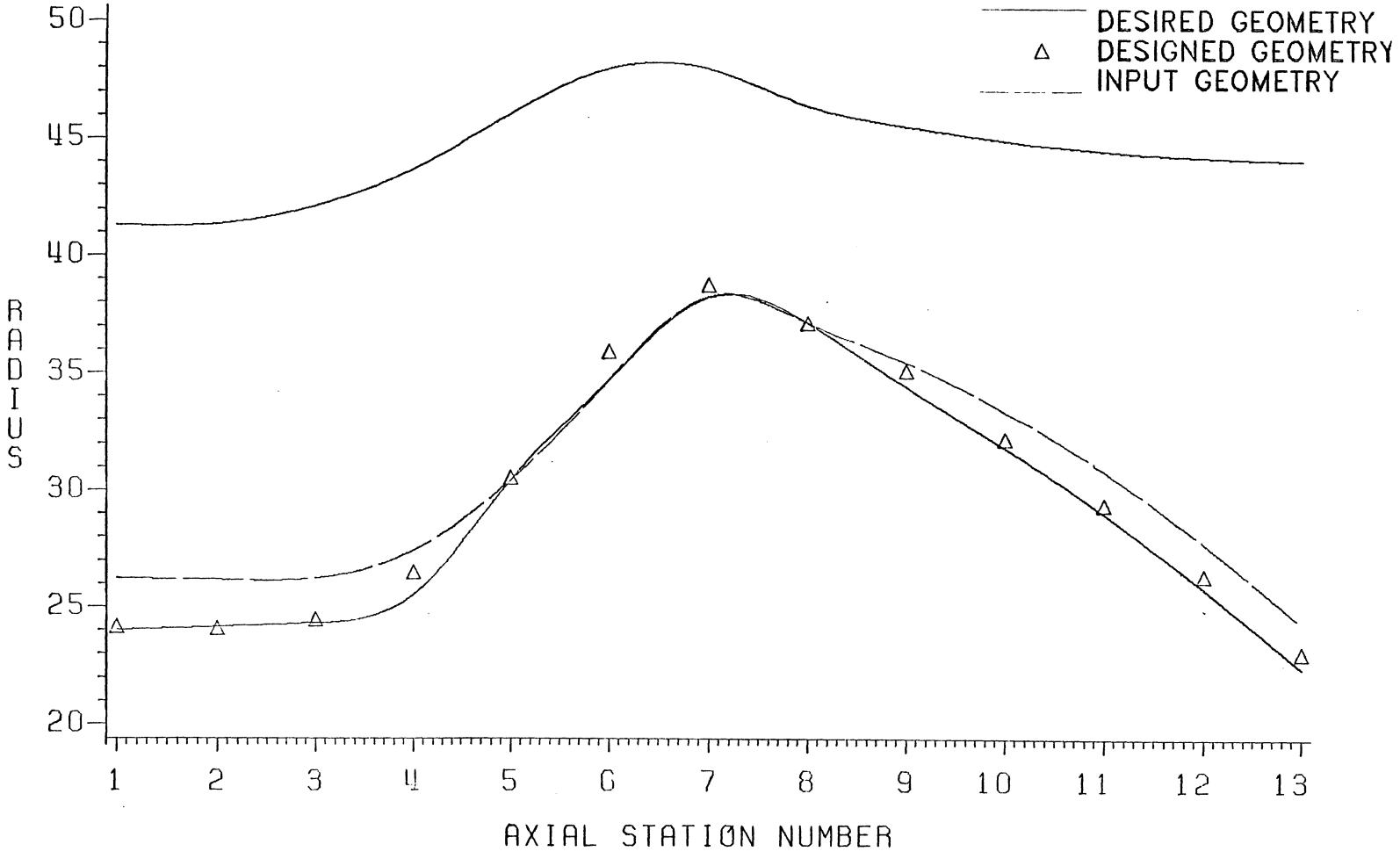

FIG.20. INNER WALL DESIGN OF BYPASS DUCT (CASE 7)

gence criterion for stopping the relaxation process, which is described in section 2.1 was changed. Specifically, in both analysis and design calculations, it was reduced to a maximum change of Mach number of less than 0.01 (rather than .001). It was observed that such reduction of Mach number convergence criterion could decrease the number of nozzle iterations to less than 130. With these changes in program, test case eight was run with a displacement under-relaxation factor of 0.4. The displacement was specified at the throat (similar to case 7). The program ran for 68 seconds and stopped after completion of seven design calculations. The pressure distribution did not converge to the desired one. However, the result as shown in Fig. 22 is very close to the desired pressure distribution. It can be seen that the designed geometry deviates from the N6 geometry at the inlet and the converging portion of the duct, but after the throat, the diverging portion is well predicted.

4.3 Important Comments

There are two important comments that should be added to clarify some aspects of the above test cases. First is the proper selection of the displacement relaxation factor. As mentioned earlier, some cases will converge with under-relaxing and some will converge with over-relaxing the calculated displacements. Unfortunately, no logical trend for proper selection of these factors has been found. A case which runs successfully with an under or over-relaxation factor of 0.10 may or may not be successful with a factor of 0.40 or vice versa. Nevertheless, the author feels obliged to explain his personal trial and error experiences, hoping that such explanation will be helpful. Basically, each test case is started with a high value (0.4) of under-relaxation

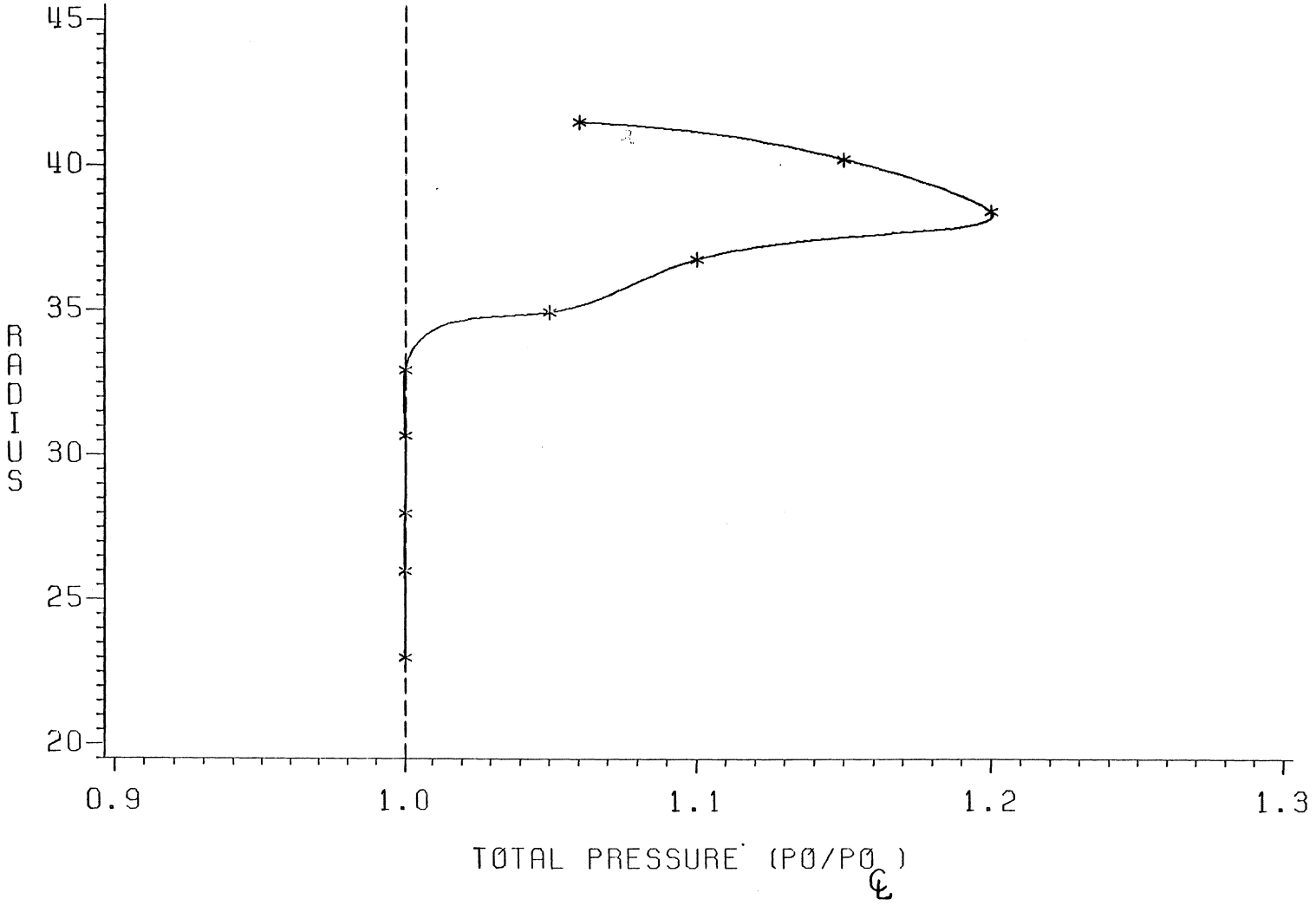

FIG.21. INLET TOTAL PRESSURE VARIATION (CASE 8)

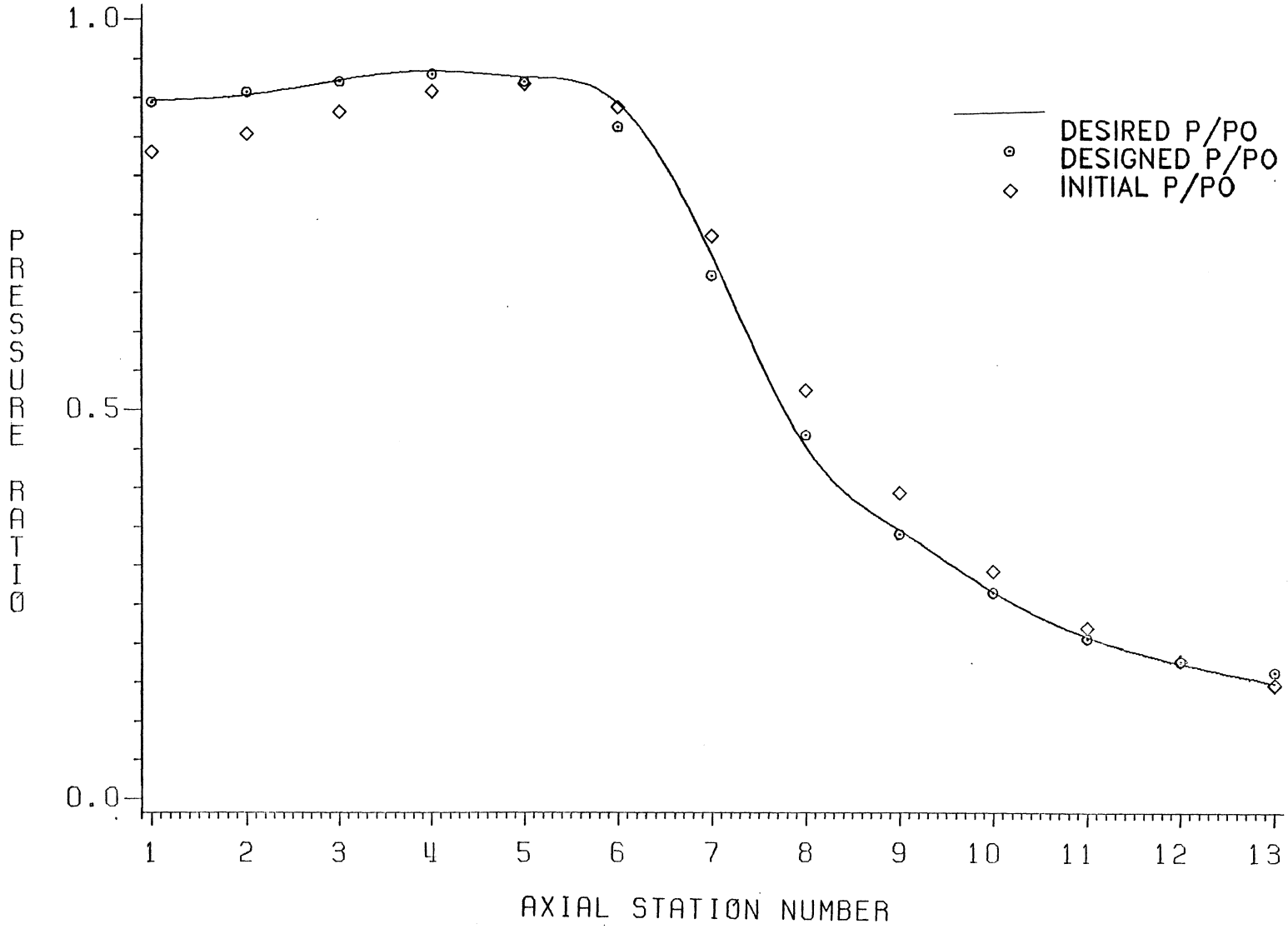

FIG.22. INNER WALL PRESSURE DISTRIBUTION OF BYPASS DUCT (CASE 8)

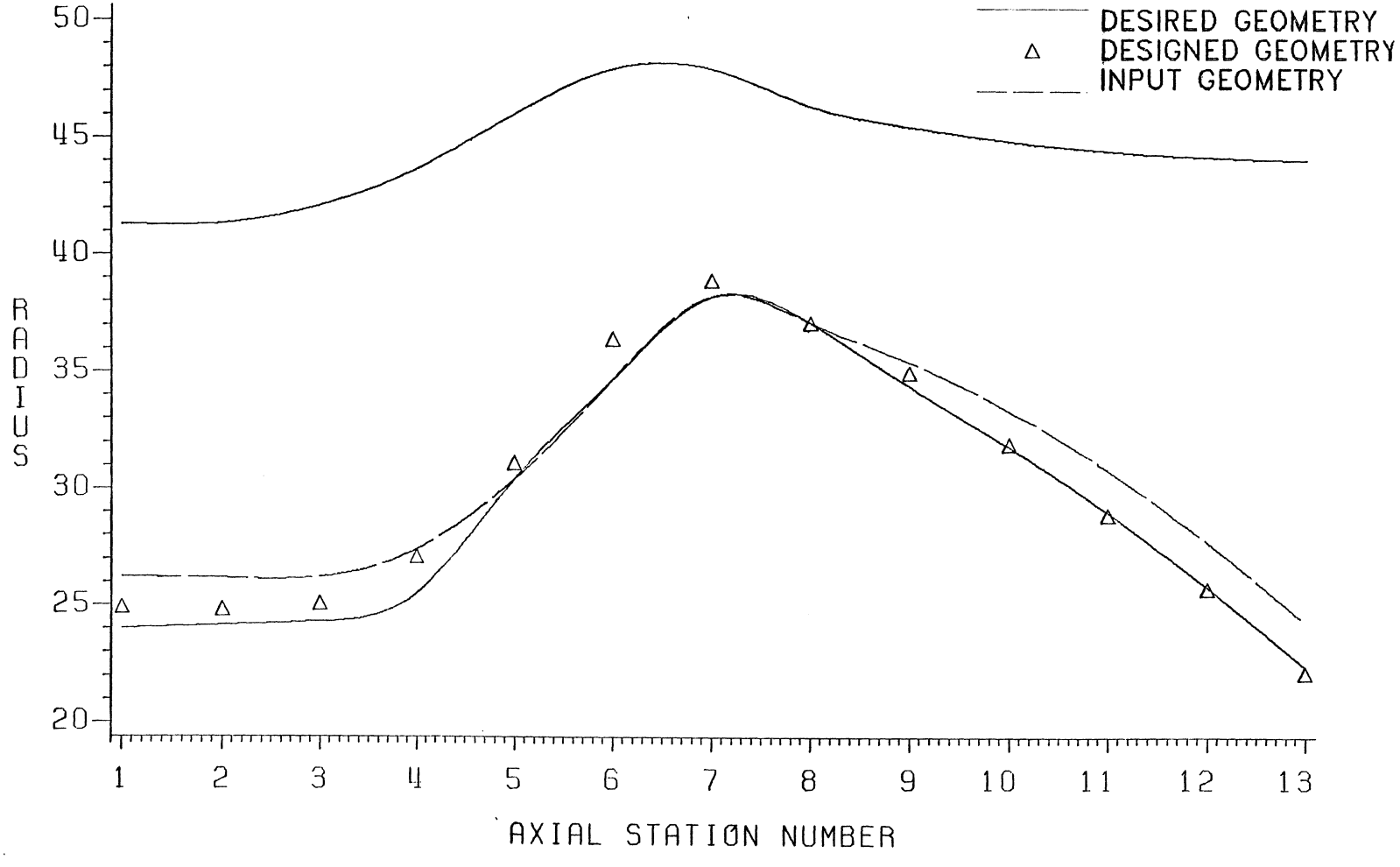

FIG.23. INNER WALL DESIGN OF BYPASS DUCT (CASE 8)

factor. If convergence is not obtained, the results are checked. If a gradual damping of displacements is observed, then this factor is reduced (say, to 0.2) and another case is run. If still the same behavior of the displacements is observed and convergence is not obtained, then a value of zero is tried and after that small over-relaxation values should be tried. However, if anytime between these tests the results reveal an over-shooting (over-shooting can be determined if displacement of two successive design calculations change sign), then intermediate values of the relaxation factor should be tried. In most cases, fewer than three trials are made before the proper value is guessed.

The second aspect of the test cases requiring additional comment is associated with the rotational flow effects. As a result of one converged and one unconverged test case it was discovered that small values of rotation function, F, in the vicinity of the centerbody were needed. A large value of rotation function near the centerbody violates the assumption upon which Eq. 2.8 is based. To prevent any difficulty caused by F, it was necessary to specify nearly constant values of total pressure near the centerbody for both cases six and eight which can be seen in Fig. 15 and 21.

5. CONCLUSIONS AND RECOMMENDATIONS

The design calculation described here is capable of designing exhaust nozzles with a prescribed pressure distribution. The ability of the method to design nozzles with various pressure distributions is tested and numerous results are obtained to prove the validity and reliability of the calculations. A complete nozzle wall can be designed or a given wall can be modified to produce a desired pressure distribution. In its present form, the program can be considered as a computational method which is reliable, economical in computer time, and gives good engineering accuracy.

Propulsion nozzles are predominantly converging in shape particularly in commerical aircraft applications. Therefore, this technique needs to be incorporated into a convergent nozzle program which includes the effects of the freestream. A program to carry out the analysis calculation of such nozzles is currently under development.

Although the program in its present form is efficient in terms of computer time, modifications can be made to increase the computational speed. Using an optimum relaxation factor in the relaxation process for the velocity function is an example of such a modification. Another technique to be considered is to control the relaxation process of the iteration loop contained in Brecht's (7) program so that fewer cycles take place for each design calculation. Insisting on complete convergence of Brecht's method for each design calculation is needlessly wasteful in terms of computer time.

6. APPENDIX

6.1 Flow Chart

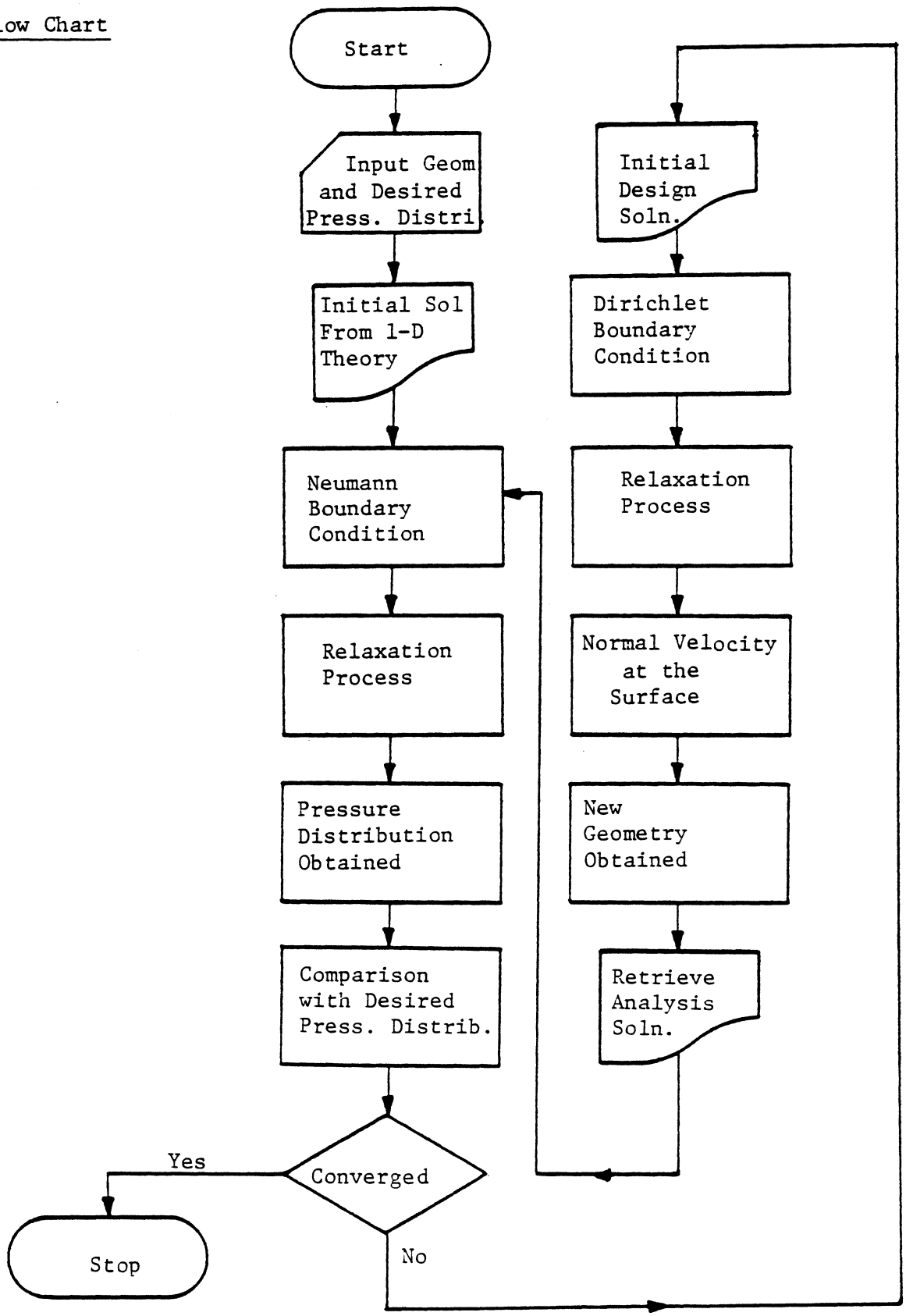

7. REFERENCES

1. Brown, E. F., and G. L. Hamilton, "A Survey of Methods for Exhaust-Nozzle Flow Analysis," AIAA Paper No. 75-60, 1975.

2. Brown, E. F., T. J. F. Brecht, and K. E. Walsh, "A Relaxation Solution of Transonic Nozzle Flows Including Rotational Flow Effects," Journal of Aircraft, October, 1977, Vol. 16, No. 10, pp. 944-951.

3. Murman, E. M., and J. D. Cole, "Calculation of Plane Steady Transonic Flows," AIAA Paper No. 70-188, 1970, pp. 15-20.

4. Murman, E. M., "Computational Methods for Inviscid Transonic Flows with Imbedded Shock Waves," Flight Sciences Laboratory, Boeing Scientific Research Laboratories, February, 1971.

5. Jameson, A., "Iterative Solution of Transonic Flows Over Airfoils and Wings, Including Flows at Mach 1," Communications on Pure and Applied Mathematics, Vol. 27, 1974.

6. Walsh, Keven E., "An Application of Relaxation Methods to Transonic Nozzle Flow," Master's Thesis, Mechanical Engineering Department, Virginia Polytechnic Institute and State University, Blacksburg, Virginia, September, 1974.

7. Brecht, T., "A Relaxation Method for the Solution of Rotational Transonic Nozzle Flow," Master's Thesis, Mechanical Engineering Department, Virginia Polytechnic Institute and State University, Blacksburg, Virginia, August 1975.

8. Tranen, T. L., "A Rapid Computer-Aided Transonic Airfoil Design Method," AIAA Paper No. 74-501, June, 1974.

9. Henne, P. A., "An Inverse Transonic Wing Design Method," AIAA Paper No. 80-0330, January, 1980.

10. Carlson, L. A., "Transonic Airfoil Analysis and Design Using Cartesian Coordinates," Journal of Aircraft, Vol. 13, May, 1976, pp. 349-356.

11. Volpe, G., "The Inverse Design of Closed Airfoils in Transonic Flow," AIAA 21st Aerospace Science Meeting, Reno, Nevada, January, 1983.

12. Shapiro, A. H., The Dynamics and Thermodynamics of Compressible Fluid Flow, Ronald Press Co., New York, 1953, p. 282.

13. Roache, P. J., Computational Fluid Dynamics, Hermosa Publishers, Albuquerque, New Mexico, 1972, pp. 290-302.

The vita has been removed from the scanned document